The Effect of Lubrication System and Marine Specific Factors

on Diesel Engine Emissions

by

Ronald B. Laurence Jr.

Bachelor of Science in Naval Architecture and Marine Engineering
United States Coast Guard Academy
(1990)

Submitted to the Department of Ocean Engineering and the Department of Mechanical Engineering
in Partial Fulfillment of the Requirements for the Degrees of

Master of Science in Naval Architecture and Marine Engineering

and

Master of Science in Mechanical Engineering

at the
Massachusetts Institute of Technology
May 1994

Signature of Author_____

Certified by_____
Alan J. Brown
Professor, Department of Ocean Engineering
Thesis Advisor

Certified by_____
Dr. Victor W. Wong
Department of Mechanical Engineering
Thesis Advisor

Accepted by_____
A. Douglas Carmichael
Chairman, Departmental Graduate Committee
Department of Ocean Engineering

Accepted by_____
Ain A. Sonin
Chairman, Departmental Graduate Committee
Department of Mechanical Engineering

(This page intentionally left blank)

The Effect of Lubrication System and Marine Specific Factors on Diesel Engine Emissions

by

Ronald B. Laurence Jr.

Submitted to the Department of Ocean Engineering and the Department of Mechanical Engineering in Partial Fulfillment of the Requirements for the Degrees of Master of Science in Naval Architecture and Marine Engineering and Master of Science in Mechanical Engineering

ABSTRACT

A two-part diesel engine emissions study was conducted.

The first part studied the effects of lubricant parameters on particulate emission rate and composition. A scaled down constant volume sample (CVS) dilution tunnel was constructed. Engine load, viscosity and top ring gap width were chosen as variables. Fifteen tests were run for each of three lubricant conditions: 10W-30 with standard ring configuration, 15W-40 with standard ring configuration, and 15W-40 with an enlarged top ring gap. Each fifteen test group included five tests each at three operating conditions.

Samples were collected on 47mm Teflon coated filters. Each sample underwent a soxlet extraction to determine soluble organic fraction (SOF) and a unique gas cromatograph method to determine per cent lubricant contribution to the SOF. Particulate rates were highest with lower viscosity and larger top ring gap. At high load, the difference in particulate rate was due to changes in the non-soluble portion, while at medium and low loads, the change in particulate rate was due to differences in the lubricant derived portion of the SOF. In addition, changes in the fuel derived portion of the SOF were discovered and attributed to changes in the amount of fuel absorption in the oil film.

The second part studied the effect of aqueous exhaust injection on gaseous emissions. To simulate a common marine exhaust configuration, an apparatus was constructed whereby water is injected into the diesel engine exhaust. Gaseous emissions were measured upstream and downstream of injection. No significant differences were discovered in the concentrations of oxygen, carbon monoxide, or oxides of nitrogen in the altered exhaust. Visual inspection of water samples, however, indicate that a significant amount of particulates are captured by the injected water and presumably flushed into the body of water in which the ship is operating.

Thesis Supervisor:	Victor W. Wong
Title:	Lecturer, Department of Mechanical Engineering
Thesis Reader:	Alan J. Brown
Title:	Professor of Naval Construction and Engineering

(This page intentionally left blank)

ACKNOWLEDGMENTS

Many people have contributed to the success of this project. This author wishes a sincere thank you to them all. First I want to thank my Thesis advisors, Dr. Victor Wong and Prof. Alan Brown, for their guidance, patience, and editorial comments. Their leadership has always kept me well on track. I also want to especially thank Prof. Brown for always being concerned for my best interest.

I also wish to thank Dr. Alan Bentz of the U. S. Coast Guard Research and Development Center, one of the project sponsors. Dr. Bentz was much more than just a sponsor. I very much appreciate his guidance and technical advice along the way.

The staff in the Sloan Automotive Lab have provided indispensable assistance. Brian Corkum's help and advice was irreplaceable; I could never have built an apparatus without him. Joan Kenny's administrative support and general assistance was also especially significant. Joan was always there. In addition, I wish to thank Don Fitzgerald for always being able to answer the "tough" questions.

For social support and assistance, I must thank my fellow students in the lab. It was working with these people who made it fun and worthwhile. I especially thank Janice, for never being short of lively conversation, Mark, for always being ready to help and talk, and Goro, Tian, Mike, Gatis, Richard, and Peter (among others), for all their help and insight. They are all true friends.

Of course, I must thank my fellow Coast Guard Officers, Pat, Doug, Dan, Eric, and Rob, for always providing a reason to take a long lunch.

Additionally, many people played small but significant roles in the project. John Lopatynski and Ortech Corporation provided great service and chemical analysis (not a small role). Mr. Flaherty at Cummins Engine also provided necessary analysis and was gracious enough to share his analysis technique. Dave Fiedler and Dana Corporation

provided excellent ring-altering services. Philip Burnett of Shell Oil provided technical suggestions and lubricant information. Jerry Payne of Caterpillar supplied me vital information about the 3412 engines. Finally, Sue Blood, from the U.S. Coast Guard Pacific Area Maintenance and Logistics Command, went out of her way to ship me significant exhaust parts from a Coast Guard Cutter. I thank them all for their help.

Finally, as always, I thank my wife and family for their tolerance, guidance, and encouraging pushes along the way. I couldn't (or wouldn't) have done it without them.

This work has been supported by the Consortium on Lubrication in Internal Combustion Engines, whose members include Dana Corporation, Pennzoil, Peugeot, Renault, and Shell Oil Company, and by the United States Coast Guard.

R. B. Laurence Jr.
6 May 1994

TABLE OF CONTENTS

LIST OF FIGURES

(This page intentionally left blank)

LIST OF TABLES

(This page intentionally left blank)

NOMENCLATURE

Symbol	Definition	Units
a	# of carbon atoms per fuel molecule	
b	# of hydrogen atoms per fuel molecule	
[CO2]dil	carbon dioxide concentration in dilute exhaust	%
[CO2]raw	carbon dioxide concentration in raw exhaust	%
f_{mix}	mixing factor	
$\dot{m}_{ex}$	total exhaust mass flowrate	g/s
$\dot{m}_a$	intake air mass flowrate	g/s
$\dot{m}_s$	sample mass flowrate	g/s
$\dot{m}_{H_2O}$	injected water mass flowrate	g/min
m_f	final filter mass	g
m_i	initial filter mass	g
m_p	total particulate mass	g
m_{st}	total sample mass	g
MW_a	air molecular weight	
MW_{ex}	exhaust molecular weight	
MW_{H2O}	molecular weight of water	
P	power	hp
r_D	dilution ratio	
R_a	actual removal rate of NO	ppm

R_m	maximum(saturated) removal rate of NO	ppm
t	sample time	s
$Ta = \mu U/\sigma$	Taylor Number	
TPR	total particulate rate	g/bhp-hr
U	average velocity of blowby gas over oil puddle	m/s
V_t	total sample volume	L
$\overline{x}$	saturated mole fraction of NO in water	
$\dot{x}_{NO}$	saturated mass flowrate of nitric oxide	mol/min
ρ_s	sample density	kg/m^3
ρ_{ex}	exhaust density	kg/m^3
σ	surface tension	N/m
ρ_a	air density	kg/m^3
μ	dynamic viscosity	$N\text{-}s/m^2$
λ	relative air to fuel ratio	

Chapter 1 INTRODUCTION

Emissions from diesel engines play a major role in the deterioration of air quality. Be it from automobiles, trucks or ships, the aggregate effect of even low emission levels can have a marked effect on the health of humans and the environment. This study encompasses two separate parts, each with the objective of better understanding the factors influencing the rate and composition of these emissions. The first section deals with the effects that lubricant and lubrication system parameters have on diesel particulate emissions in any general application. The second section deals with the emissions from a diesel engine in a marine application, specifically investigating the effect of aqueous exhaust injection, commonly used on ships as an exhaust cooling measure.

SECTION 1: PARTICULATE STUDY

Chapter 2 BACKGROUND

2.1 Previous Research

Diesel particulates are commonly defined as any exhaust material, except water, that can be collected on a filter at a temperature below 53°C [1]. Predominantly, they are composed of a carbon core with a complex collection of absorbed hydrocarbons and inorganic compounds which have condensed on the surface [2]. It is the collection of condensed compounds, particularly the carcinogenic polynucleic aromatic hydrocarbons (PAH), which may create the most significant health risks [1], [3]. Using traditional analysis, these soluble organic compounds can be extracted and the soluble organic fraction(SOF), the soluble organic percentage of the total particulate mass, can be determined [1].

Clearly, it is desirable to reduce not only the total particulate rate, but the harmful carcinogenic compounds found in the SOF. In conjunction with the U. S. Clean Air Act Amendments of 1990, the U. S. Environmental Protection Agency(EPA) has set strict standards for the reduction of particulate rates. Most significantly, they have set a 1994 heavy-duty vehicle standard of 0.10 g/bhp-hr and a 1996 urban bus standard of 0.05 g/bhp-hr [1], [3]. In addition, the California Air Resources Board has recently considered lowering the acceptable heavy duty vehicle standard to 0.05 g/bhp-hr [3]. To meet these standards, engine manufacturers and fuel and oil suppliers have found it necessary to reduce all sources of particulates.

Diesel particulate emissions are partially lubricant derived [4], [5], [6]. It is therefore desirable to investigate the sources, causes and factors surrounding the oil

contribution. The composition of the particulate mass and the rate of particulate emission are influenced by a number of factors. A significant fraction of the SOF is derived from the lube oil, while the carbonaceous particulate core and inorganic constituents are largely fuel derived [7], [8]. Dowling [6] found that particulate rate increases with decreasing viscosity and increasing volatility. In addition, he concluded that oil contribution increases with increasing speed and decreasing load. Andrews et.al. [9], found that there is also significant influence of oil age which is caused by fuel dilution and carbon thickening, thereby altering the oil viscosity.

Indeed, particulate rate is also related to oil consumption. Zelenka et. al. [10] and Essig et. al. [7] display that the emission rate of oil derived particulates is directly proportional to the oil consumption rate. They further conclude that reduction of cylinder wall oil consumption, the main source of lubricant derived particulates, should be a primary focus in reducing overall particulate mass.

Experimental data show that oil film thickness increases with decreased viscosity [11]. This could indicate that lower viscosity oils leave more residual oil on the liner, therefore explaining an increase in particulate rate with decreased viscosity.

The puddle theory of oil consumption describes an oil consumption mechanism whereby a small amount of oil is blown into the combustion chamber through the top ring gap when the cylinder pressure drops below the inter-ring pressure during expansion [12]. If this is a major source of oil consumption and oil derived particulates, it follows that an increase of ring gap width will also significantly increase the total particulate rate through the oil contributed portion.

2.2 Purpose

The first part of this study focused largely on developing a particulate sampling system in the Sloan Automotive Laboratory, a prerequisite to further particulate studies. Design, construction, and operation of a particulate sampling system, including a dilution tunnel, was the major concern. Having obtained reasonable and repeatable results, this study attempts to support the previous work on the effects of lubricant viscosity and load on total particulate rate, SOF, and oil derived particulate fraction. In addition, a piston ring parameter, specifically the top ring gap, was also varied to study its effect on particulate fractions. The results should further reinforce the relationships between oil consumption and particulate emissions, while giving additional credence to the puddle theory of oil consumption. Finally, this project is a precursor to further oil consumption and particulate experiments, including a possible study which directly measures oil consumption and collects particulates simultaneously using radioactive tagging.

Chapter 3 EXPERIMENTAL APPARATUS

3.1 Engine

The experimental engine used was a single cylinder Ricardo/Cussons standard Hydra engine connected to a Dynamatic Model 20 AC dynamometer with a Digilog controller. Details of the engine are given in Table 3-1.

MANUFACTURER:	G. CUSSONS LTD.
MODEL:	HYDRA RESEARCH ENGINE
NUMBER OF CYLINDERS:	1
DISPLACEMENT:	0.45 L
BORE:	80.26 MM
STROKE:	88.9 MM
MAXIMUM SPEED:	4500 RPM
MAXIMUM POWER:	8 KW
MAXIMUM CYLINDER PRESSURE:	120 BAR
COMPRESSION RATIO:	20:1
INJECTION:	DIRECT

Table 3-1 Engine Characteristics

Fueling is normally manually controlled by a servo motor which acts as the rack actuator. The motor is controlled by a sensitive dial at the control panel via an electronic feedback mechanism. Unfortunately, the servo card failed early in the experiments,

forcing the operator to manually move and set the actuator cable. Quick, repeatable setting of the rack, therefore, became difficult. During experimentation, a speed set point was chosen and the dynamometer altered the load automatically to maintain speed.

Injection timing settings were manually controlled by the operator. For this study, the timing was changed with engine speed to the value recommended by the manufacturer to be "optimum" [13].

The piston has a three ring configuration, i.e., two compression rings and an oil control ring. It was the top compression ring that was altered for this study.

The engine is fully instrumented. Oil, coolant, air, and exhaust temperatures were monitored at various locations. This monitoring allows the experimenter to insure constant conditions between tests. Engine speed is measured by a magnetic pick-up mounted at a .020" interval from a 60 tooth gear on the drive shaft. Engine load is measured by a load cell mounted at a fixed distance from the drive shaft axis between the dynamometer and test bed. Both the oil and coolant are both pumped, and can be heated, electrically, allowing great flexibility of temperature and ease of flushing.

3.2 Sampling System

The particulates were collected using a scaled down version of a constant volume sample (CVS) dilution tunnel and system similar to that described by Wong et.al [14]. A diagram of the system is shown in Figure 3-1. Compressed air is supplied through a 2" line from large shop compressors. A 2" Balston A15/80-DX filter is installed upstream of the tunnel to remove oil and moisture from the air. The stated removal effectiveness of this filter is 93%. As a background test, a sample of air was drawn through the particulate system with the engine off to determine if this filter sufficiently cleaned the air. No measurable material collected on the particulate filter after a one hour test.

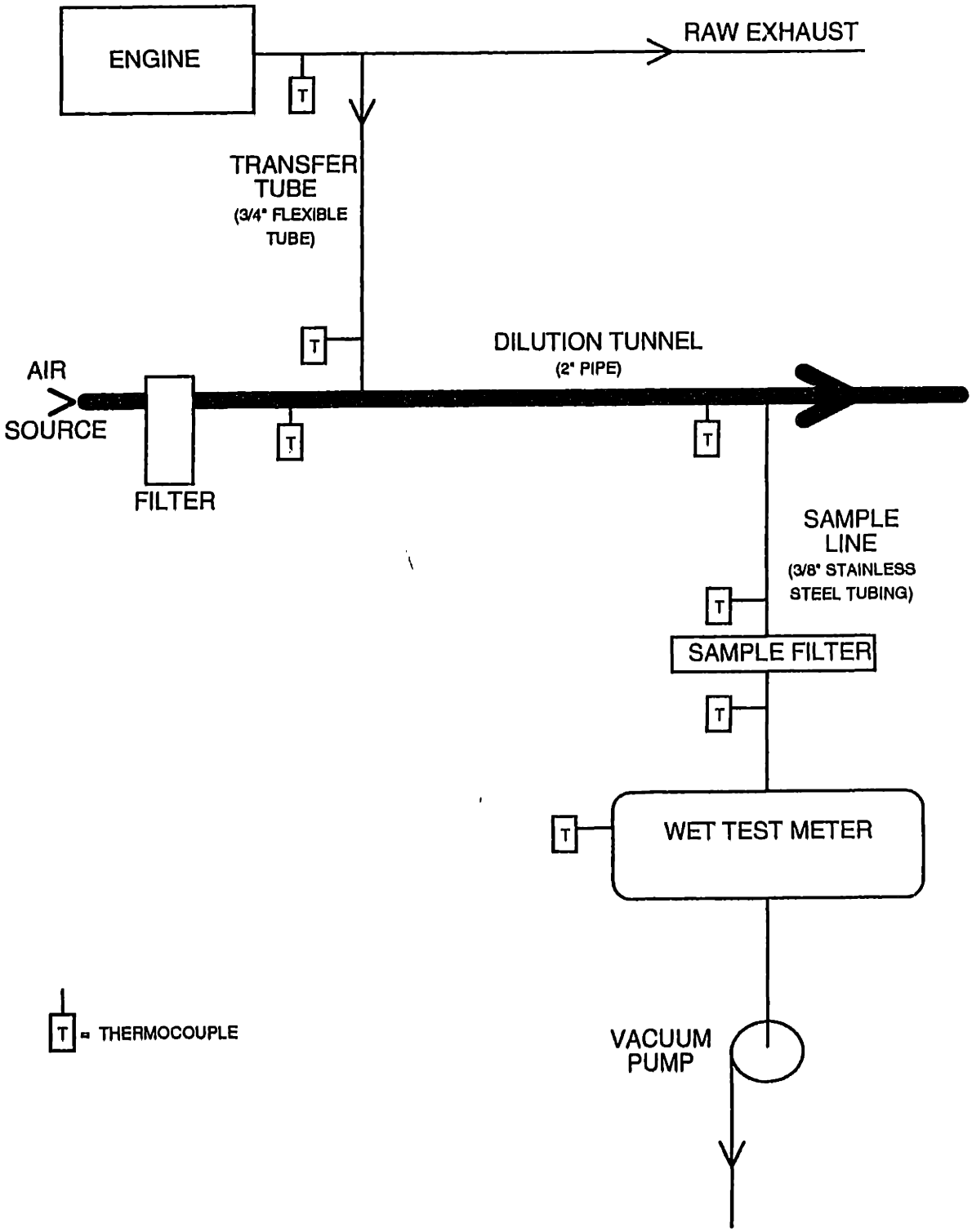

Figure 3-1 Particulate Sampling System

After filtration, the air enters the 2" pipe dilution tunnel. An exhaust sample is drawn into the tunnel through a 3/4" flexible transfer tube using a venturi powered by the dilution air. The transfer tube is connected to the main 2" raw engine exhaust line. The air and exhaust are mixed over an approximately 3' tunnel length. The diluted sample is then drawn through the filter and wet test meter. The sample line is 3/8" 316 stainless steel tubing. Pallflex Teflon coated 47 mm fiber filters, P/N TX40HI20WW, are used to collect the sample, and are mounted in a Graseby Anderson 316 Stainless Steel filter holder, P/N SE273. The sample line can be isolated from the dilution tunnel by an installed high temperature stainless steel ball valve. After filtration, the sample is drawn through a wet test meter manufactured by Precision Scientific Petroleum Instruments Company. This meter measures total volumetric flow of the sample. A positive displacement vacuum pump draws the sample through the sample line.

Dilution ratio is measured by sampling the CO2 concentration of the exhaust before and after dilution. The specific characteristics of the gas sample line and CO2 analyzer will be discussed later in sub-chapter 10.3.

Temperatures can be measured at various locations in the sampling system. Most importantly, thermocouples are located before and after the filter enclosure to insure that the sample is below 51.7°C [15], thereby allowing sufficient hydrocarbon condensation. Temperatures of the transferred exhaust, incoming air, and diluted air can also be measured. The transfer tube is insulated with a high temperature fiber "exhaust blanket." Otherwise, the system was not insulated. As a result, there are significant heat losses to the environment. In some cooler conditions, dilution is not necessary as sufficient cooling occurs from the losses alone.

To reduce the possible catalytic effects, the dilution tunnel and sampling lines are mild or stainless steel. All components of the system were cleaned with a de-greasing

agent and dried before construction. Care was taken to minimize or eliminate any thread compounds from residing on the inside surface of the tunnel. Before testing, the engine was run at its hottest condition without dilution air to oxidize any possible remaining contaminants.

Chapter 4 EXPERIMENTATION

4.1 Test Procedure

The particulate filters were conditioned and weighed to 10 μg by a commercial test laboratory and shipped for testing [16]. In addition, each filter was weighed in the engine laboratory to 100 μg. The filter was then placed in the filter holder and wrench-tightened to avoid O-ring bleed. Starting sample volume was recorded. After the engine was settled at the proper operating condition, the test began by opening the sample line isolation valve, starting the vacuum pump, and recording the time. The dilution air remained on whenever the engine was running to keep the temperatures stabilized. Other pertinent data was recorded while the sample was being collected. At the end of the sample interval, the isolation valve was closed, the vacuum pump secured, and the final readings taken. The filter was immediately weighed, packaged in double sealed plastic bags and cooled to refrigerator temperature (4°C). The samples were then shipped to the analysis laboratory. While weights were recorded in the engine laboratory, only values obtained by the analysis lab were used, as the samples were post-conditioned prior to final weighing. Immediately after packing the sample, the engine load was changed in preparation for the next test.

Between each round of fifteen tests, the lubricant or top ring was changed, as these were the two primary variables in the experiment. Oil changes were completed using a fill-flush-fill technique. Old oil was heated to 80°C and drained from the sump. The discharge line from the oil pump was then disconnected and re-routed into a collection vessel. Per manufacturer's recommendation, the pump was then turned on and allowed to suck all remaining oil out of the sump [13]. The oil system was then reassembled. The engine was then filled with new oil of the same viscosity as the replacement oil. It was

heated to 80°C and pumped through the system as the engine was motored at 1200 RPM for 15 minutes. The same technique was then used to drain and pump out this flushing oil. With the sump dry, the filter was changed and the engine re-filled with the new oil. After each change, the engine was run at 3000 RPM and high load for 5 hours per the findings of Hartman [17] that most volatility reduction in new oil occurs during the first five hours of high temperature operation.

The top ring was changed by removing the piston through the top of the liner. The three ring gaps were oriented at 120 ° from each other to minimize the possibility that the gaps would align, thereby increasing blow-by.

4.2 Controls

Results from initial experiments indicated poor repeatability among tests with identical conditions. Coupled with the small emissions changes associated with variable viscosity, additional control measures were employed to maximize repeatability and minimize the effects of inadvertent variables. These efforts are addressed in the following paragraphs of this section.

Because the rack positioner was damaged, each operating condition was determined by torque, fuel flow, and exhaust temperature. While the three values did not always agree with previous tests, the condition was repeated as well as possible by considering each of the three readings.

Temperature was a major consideration. At the beginning of each day, the engine was warmed for one hour prior to beginning tests. Oil temperature, exhaust temperature, and the temperatures throughout the sampling system were allowed to stabilize after each load change. Oil temperature changed slightly for each condition, but was normally about 70°C.

Build-up of particulate in the sampling system was also a concern. The dilution air was on whenever the engine ran to minimize buildup in the tunnel (This also served to keep the tunnel temperature stable). Between each test, the sample line was blown out with compressed air to eliminate clogging and remove any build-up from previous tests. In addition, between each third test, the engine was run at 3000 RPM at high load for five minutes to remove any carbon buildup in the engine from extended running at the lower load conditions. During the ring change, the piston, liner and head were not cleaned, i.e., no carbon build-up was removed, so as to reduce any variability created by the sudden absence of long term carbon or hydrocarbon build-up.

At the beginning of testing, the compressed air regulating valve was fixed to an open position where it remained for the entire testing period. This step was taken to remove any variability that may have been created by inaccurate CO2 sensing or dilution ratio measurement. All tests had an identical volumetric dilution air flow through the tunnel. Sampling times were also constant at twenty minutes. This was done to remove possible variability created by changes in sampling flow between the beginning and end of tests. During the 15W-40 tests, however, some sample times were increased to 30 minutes because twenty minute sample durations were not producing adequate filter loadings.

All oils used were the same production oils formulated by the same company. While the flash points were a few degrees different, the five hour run-in should have reduced it somewhat. The altered top ring was a standard production ring that was cut, as opposed to having a new ring made.

To reflect current regulatory movement and to reduce the amount of inorganic contributions to the particulate, a single batch of low sulfur (<0.05%) fuel was used for all 45 tests.

4.3 Test Matrix

Three variables were used for this study. Each test condition was run five times for repeatability. Two production oils of differing viscosity (10W-30 & 15W-40) with the

LUBRICANT	RING CONFIGURATION	ENGINE LOAD	# OF TESTS
10W-30	STANDARD	HIGH	5
		MEDIUM	5
		LOW	5
15W-40	STANDARD	HIGH	5
		MEDIUM	5
		LOW	5
15W-40	ENLARGED TOP GAP	HIGH	5
		MEDIUM	5
		LOW	5

Table 4-1 Test Matrix

standard manufacturer's ring configuration were used for the first comparison. Then, using the 15W-40, the top ring gap was enlarged for a second comparison. For each of

these three lubricant parameter conditions, the engine was tested at three loads. 45 total tests were conducted for final analysis. Table 4-1 summarizes the test matrix.

ENGINE LOAD	TORQUE (FT-LB)	FUEL FLOW RATE (CC/MIN)	EXHAUST TEMP. (° C)
HIGH(100%)	15.0	25.8	460
MEDIUM(67%)	10.0	19.8	350
LOW(33%)	5.0	15.4	270

Table 4-2 Engine Load Conditions

All tests were conducted at 2400 RPM. Table 4-2 defines the target values for the engine loading conditions.

4.4 Variable Specifics

The lubricants selected were production oils designed for diesel applications. While original intentions were to use specially formulated oils with known and controlled volatilities, logistical constraints dictated the use of production lubricants. Table 4-3 details the lubricant properties.

The rings used were those provided by the engine manufacturer. For the altered condition, the top ring cold gap was enlarged to approximately six times the standard

value. This alteration was purposely extreme to insure that the results show a significant change in emissions. The specifics of the alteration are listed in Table 4-4.

LUBRICANT	MANUFACTURER/ BRAND	VISCOSITY (CST @ 100°C)	FLASH POINT °F	POUR POINT °F
10W-30	SHELL/ROTELLA T®	10.9	405	-35
15W-40	SHELL/ROTELLA T®	14.0	415	-35

Table 4-3 Lubricant Properties [18]

INITIAL COLD RING GAP (IN)	.020
ALTERED COLD RING GAP (IN)	.119

Table 4-4 Ring Dimensions

Chapter 5 DATA AND SAMPLE ANALYSIS

5.1 Calculation of Particulate Rate

Total particulate rate was calculated from measured data to assess the effects of each of the variables on the entire particulate mass. A description of the calculation follows.

The calculation of particulate rate, normalized to power, is straightforward and governed by:

$$TPR = \frac{(m_p)(3600)}{(t)(P)} \qquad (5\text{-}1)$$

where:

TPR	=	total particulate rate (g/bhp-hr)
m_p	=	total particulate mass (g)
t	=	sample time (s)
P	=	power (hp)

While power and sample time are simple calculations, determination of total particulate mass is not, as the entire exhaust was not sampled. Calculation of the total particulate mass begins with a determination of the mass sampled.

$$m_{st} = m_f - m_i \qquad (5\text{-}2)$$

where:

m_{St}	=	total sample mass (g)
m_f	=	final filter mass (g)
m_i	=	initial filter mass (g)

The exhaust mass flowrate is then calculated from the measured fuel and intake air flowrates.

$$\dot{m}_{ex} = \dot{m}_a + \frac{(Q_f)(\rho_f)}{60} \tag{5-3}$$

where:

$\dot{m}_{ex}$ = total exhaust mass flowrate (g/s)
$\dot{m}_a$ = intake air mass flowrate (g/s)
Q_f = fuel flowrate (cc/min)
ρ_f = fuel density (kg/L)

A calculation of the sample mass flowrate will allow the determination of the ratio between the amount of exhaust passing through the filter to the total exhaust.

$$\dot{m}_s = \frac{(V_t)(\rho_s)(r_D)}{(t)(86400)} \tag{5-4}$$

where:

$\dot{m}_s$ = sample mass flowrate (g/s)
V_t = total sample volume (L)
ρ_S = sample density (kg/m^3)

Now, total particulate mass can be solved for directly with the ratio.

$$m_p = \frac{\dot{m}_{ex}}{\dot{m}_s}(m_{st}) \tag{5-5}$$

Dilution ratio and sample density also must be calculated prior to using (5-4). Dilution ratio is simply the ratio of carbon dioxide in the raw exhaust to that in the diluted sample, corrected for the concentration of carbon dioxide in ambient air.

$$r_D = \frac{[CO_2]_{dil} - 0.035}{[CO_2]_{raw} - 0.035} \tag{5-6}$$

where:

$[CO_2]_{dil}$ = dilute carbon dioxide concentration sample (%)

$[CO_2]_{raw}$ = raw carbon dioxide concentration sample (%)
0.035 = ambient carbon dioxide concentration (%)

Sample density can be now be calculated from the densities of the exhaust and ambient air. Ambient air density is proportional to absolute temperature and can be calculated directly knowing ambient temperature. Exhaust density can be calculated from the molecular weights of the exhaust and air.

$$\rho_{ex} = \rho_a \frac{MW_{ex}}{MW_a} \tag{5-7}$$

where:

r_{ex} = exhaust density (kg/m^3)
r_a = air density (kg/m^3)
MWex= exhaust molecular weight
MWa = air molecular weight

Heywood [2], provides a method to determine the molecular weight of the exhaust, given the fuel to air ratio and fuel composition. We know the overall stoichiometric combustion equation is [2]:

$$C_aH_b + \left(a + \frac{b}{4}\right)[O_2 + 3.773N_2] = aCO_2 + \frac{b}{2}H_2O + 3.773\left(a + \frac{b}{4}\right)N_2 \tag{5-8}$$

where a and b are define the carbon to hydrogen ratio in the fuel.

As the diesel runs lean, it is necessary to multiply the air reactant term by the relative air/fuel ratio and include oxygen in the equation as a product. From this, the exhaust molecular weight can be calculated directly.

$$MW_{ex} = \frac{(12)(a)+(32)(a)+(2)\left(\frac{b}{2}\right)+(16)\left(\frac{b}{2}\right)+(32)\left(\frac{\left[(2)(\lambda)\left(a+\frac{b}{4}\right)-\left((2)(a)+\frac{b}{4}\right)\right]}{2}\right)+(3.773)(28.16)(\lambda)\left(a+\frac{b}{4}\right)}{a+\frac{b}{2}\left(\frac{\left[(2)(\lambda)\left(a+\frac{b}{4}\right)-\left((2)(a)+\frac{b}{4}\right)\right]}{2}\right)+(3.773)(\lambda)\left(a+\frac{b}{4}\right)} \quad (5\text{-}9)$$

where λ is the relative air/fuel ratio.

5.2 Sample Analysis

Subsequent to testing, each filter was packaged and sent to the analytical laboratory for analysis. Samples were handled per U. S. EPA guidelines as stated in 40 CFR 86. The soluble organic portion of the sample was extracted using the soxhlet extraction method [16]. SOF was then calculated by Ortech. The soluble organic samples were then sent to Cummins Engine Company for a fuel/lube oil contribution analysis.

The fuel/lube contribution analysis was completed using a unique method developed by the Cummins Engine Co. The method is a modification of ASTM D2887 SIMDIS of petroleum products. The fractions of fuel and lube oil in the particulate sample are determined using a ratio of integrated times obtained from chromatograms of three samples: the extracted SOF, "topped" fuel, and new lube oil. (The "topped fuel" is the remainder of the fuel after 30% by volume is distilled.) The precision of lubricant derived portion of the SOF result is on the order of 0.001 g/bhp-hr [19].

Chapter 6 RESULTS

6.1 Total Particulate Rate

As predicted, mean particulate was higher using 10W-30, the lower viscosity oil, in all three loading conditions. Figure 6-1 displays this trend. The high and medium load

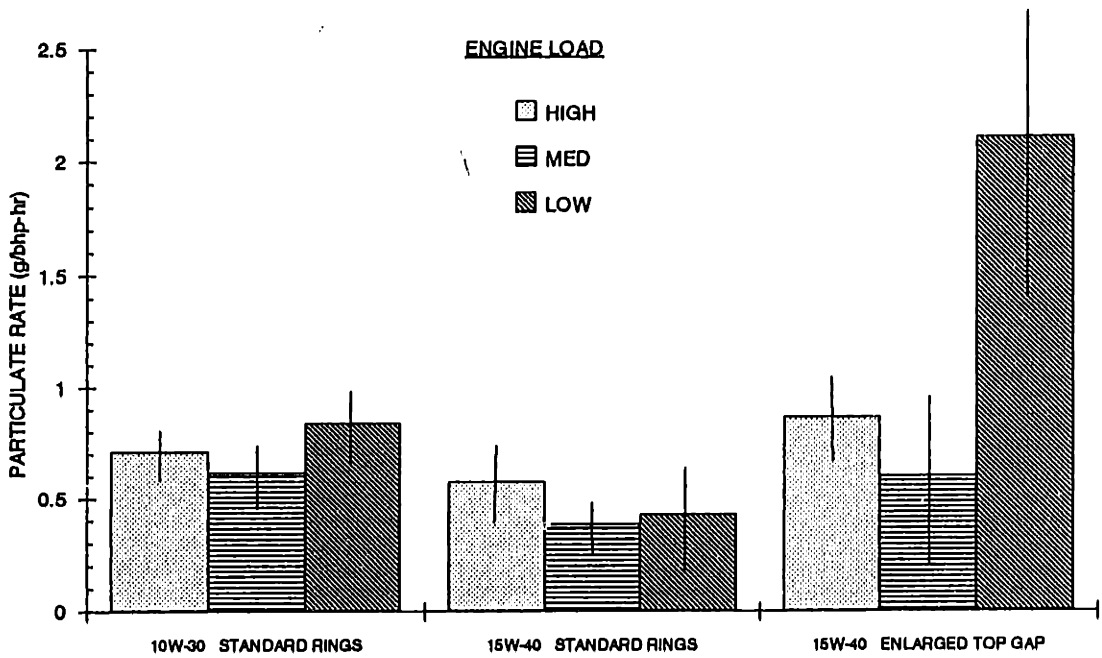

Figure 6-1 Total Particulate Rate as a Function of Lubricant Parameters for Three Engine Loads: $\pm \sigma$ Shown

conditions showed modest differences in particulate rate, while the low load condition had a more pronounced change.

With increased top ring gap, the mean particulate rate also increased for all three conditions. This result agrees with predictions and is also displayed in Figure 6-1. Note

that the variability of the particulate data was quite high, as depicted by the standard deviation range on the chart.

Variability of engine load also created a consistent difference in particulate rate. Figure 6-1 shows that the rate was highest at low load and lowest at medium load for all lubrication conditions. Individual test results are displayed in Appendicies A and B.

6.2 Particulate Composition

Consistent particulate composition trends were not clear for all operating conditions. Each condition had clearly different results. Figure 6-2 displays the mean compositions for the three lubrication conditions in the high load condition. Both the fuel and lubricant derived portion of the SOF were almost constant, while the non-soluble content increased with decreasing viscosity and increased ring gap. This does not agree with the belief that the change in particulate rate as a function of lubricant parameter is created by a change in lubricant derived soluble organic compounds. The implications are discussed in a later section.

Figure 6-3 displays the composition of the particulates from the medium load condition. In this case, the non-soluble content remains almost constant with changing lubricant parameters, while the lubricant derived portion of the SOF changes as predicted, i.e., it increases with decreasing viscosity and increasing ring gap. In addition, the fuel derived portion of the SOF increased with decreasing viscosity and enlarged ring gap.

At low load condition, the results are less repeatable, but also show increased lubricant derived SOF with increasing ring gap. Figure 6-4 illustrates the data. In addition, the fuel derived SOF also varies significantly with lubricant parameter. The data show a fuel trend similar to that of the oil. At low load, it is clear that the lubricant parameters affect the fuel composition of the particulate.

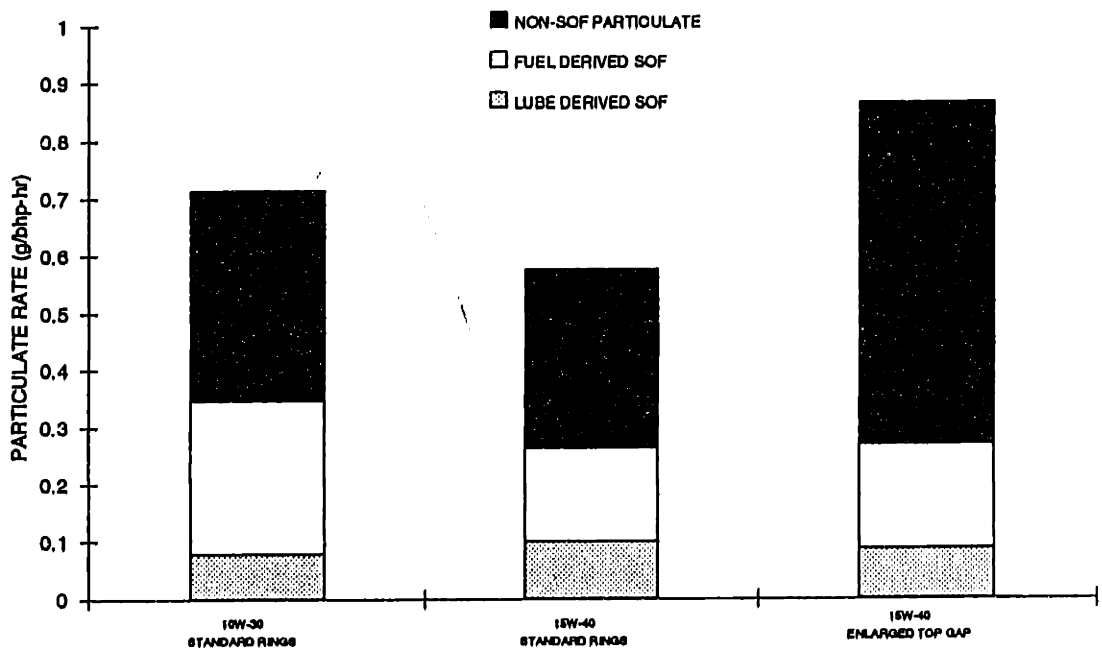

Figure 6-2 Particulate Composition as a Function of Lubricant Parameters - High Load Condition

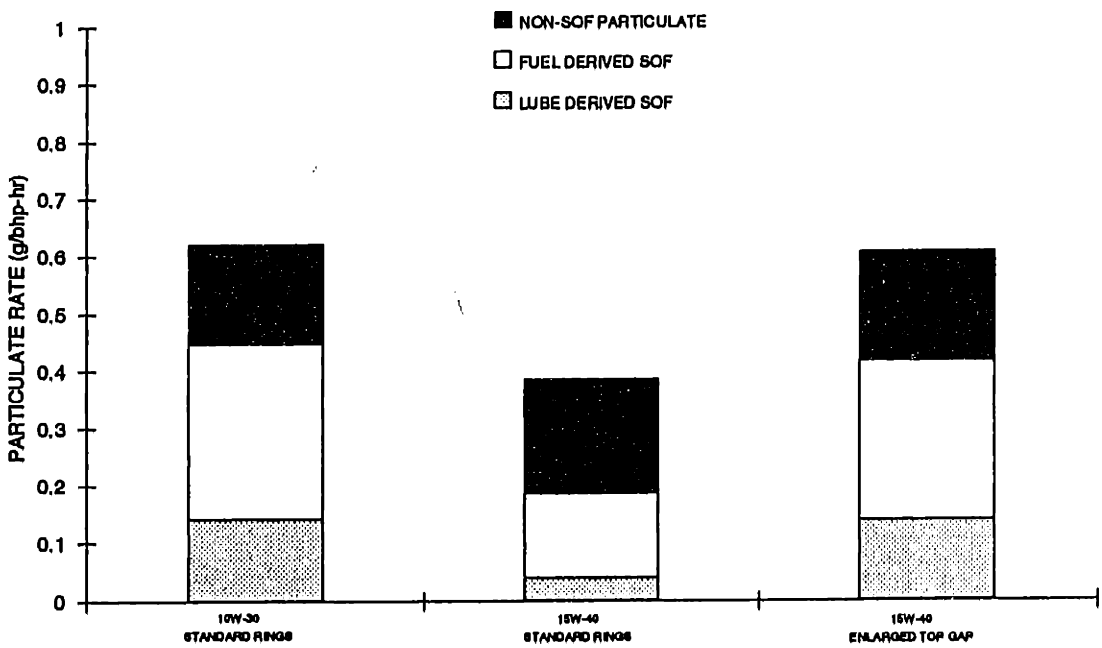

Figure 6-3 Particulate Composition as a Function of Lubricant Parameters - Medium Load Condition

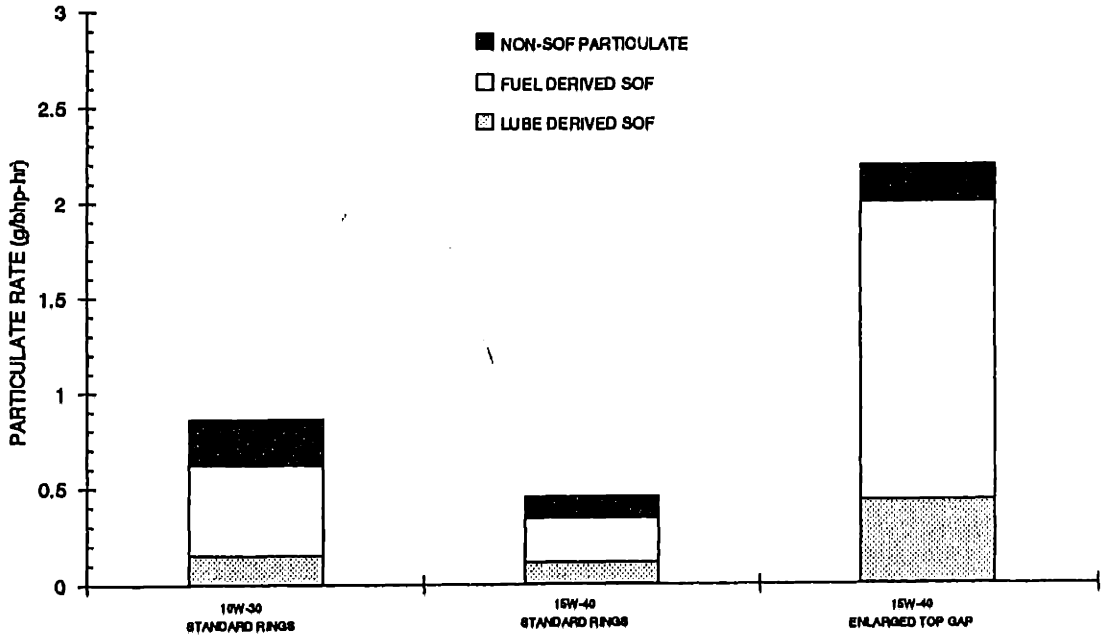

Figure 6-4 Particulate Composition as a Function of Lubricant Parameters - Low Load Condition

Chapter 7 ANALYSIS

7.1 Discussion

As predicted, total particulate rate increased with decreasing viscosity. This result is not only consistent with previous studies, but also is physically reasonable. As stated in Chapter 2, experimental data show that oil film thickness increases with decreasing viscosity [11]. Therefore, more lower viscosity oil will remain on the liner during the expansion stroke, exposing more oil to the combustion process. This additional exposure is then manifested as a higher particulate rate, as much of the oil is only partially, or not at all, oxidized.

A second argument also supports the data. According to the Puddle Theory, as viscosity decreases, Taylor Number ($Ta = \mu U/\sigma$) increases, causing an increase in puddle area. This larger puddle then increases oil consumption and particulate rate as a larger puddle enters the combustion chamber through the ring gap [12].

Similarly, total particulate rate increased with the enlarged ring gap. Again, this data agree with the predicted result. An enlarged ring gap allows a bigger puddle of oil to pass into the combustion chamber when the cylinder pressure drops below the inter-ring pressure during expansion. This increased puddle size is also manifested as an increase in particulate rate, as more oil enters the combustion chamber.

At the high load condition, the predominant change in particulate composition is the non-soluble portion. Due to both viscosity and ring configuration changes, logic dictates that the change in particulates would be due to a change in oil derived SOF, as it is the combustion of additional oil that causes the change. In the high load condition, however, this was not the case. With the hotter in-cylinder temperatures, it is quite plausible that the additional oil was partially oxidized and formed carbon. Such a process

would cause an increase in carbonaceous, or non-soluble, particulate, exactly as the data show.

At the medium and low load conditions, i.e., when the engine was running cooler, the predicted change in oil derived particulate did occur, while the non-soluble portion remained somewhat constant. These results support the conclusion that at higher loads, the additional combusted oil will become part of the carbonaceous particulate. These results also suggest the presence of a threshold temperature, above which the additional oil is oxidized instead of leaving the cylinder as altered hydrocarbon compounds.

Curiously, at all three conditions, the fuel derived portion of the SOF changed to some degree with the lubricant parameters. The changes were the same as those expected of the oil derived portion, i.e., the fuel derived SOF increased with decreasing viscosity and increased top ring gap. This data suggest that the fuel derived SOF increases when the lubricant parameters allow a stronger fuel-oil interaction. Preliminary experimental data from other studies show that some fuel is stored in the oil film during the combustion event. The fuel is absorbed during the rapid pressure increase then desorbed when the cylinder pressure decreases, thus escaping the combustion event. Additionally, the studies show more fuel absorbs with increased film thickness [20]. This phenomenon can explain the changes in fuel derived SOF as a function of viscosity, as decreases in viscosity create a greater film thickness and therefore more fuel absorption. The changes in oil formulation also may have an effect on the amount of fuel absorbed in the oil film. Increased amounts of oil in the combustion chamber, therefore, will not only create more combusted or consumed oil, but will prevent additional fuel from oxidizing.

Repeatability among experiments at the same conditions was lower that expected. while some variability was undoubtedly due to equipment issues, most were probably due to ring rotations. Schneider, et.al. [21] found that rings rotate erratically and can reach rates of 0.25 rev/min or faster in a 4 cylinder engine. While this rotation rate would

indicate that several rotations during the sample duration, the erratic and inconsistent nature of the rotations can still create variability. With the three rings rotating, relative gap orientations are changing, creating occasional situations where two or more of the gaps are aligned. Based on the findings that particulate rate is affected by ring gap parameters, it can be concluded that ring rotation can have a significant effect on particulate rate.

Such rotation probably contributed to the repeatability difficulties. Pinning the rings or using a multi-cylinder engine could reduce the variability in the data. Combined with system improvements that will be discussed in the next chapter, variability could be greatly reduced.

7.2 Conclusions

The results indicate that lubricant viscosity and top ring gap width do have a significant effect on diesel particulate emissions. Various specific conclusions can be drawn from the results and are summarized as follows:

1) Total particulate emission rate increases with decreasing viscosity. This effect is due most likely due to two mechanisms. First, the decreased viscosity leaves a thicker film on the liner during and after the expansion stroke, allowing more oil to participate in the combustion event. Second, decreased viscosity allows a larger puddle of oil to pass through the ring gap when the cylinder pressure falls below the inter-ring pressure, again allowing more oil into the combustion chamber.

2) Total particulate emission rate increases with an increased ring gap width. This result is also derived from the "Puddle Theory" mechanism, whereby oil passes through the ring gap and is consumed when the cylinder pressure falls below the inter-ring

pressure. The results of this study serve to further confirm the presence of this mechanism and the significant effect it has on oil consumption and emissions.

3) At hotter conditions, the extra oil present in the combustion chamber due to changes in a lubricant parameter is mostly partially oxidized and emitted as carbonaceous material. At cooler conditions, most of this extra oil remains in some hydrocarbon form and is eventually condensed on the particulate, thereby contributing to the oil derived SOF.

4) Changes in lubricant parameters affect not only oil derived emissions, but fuel derived emissions as well. Through the process of fuel absorption and desorption, increased oil on the liner prevents additional fuel from participating in the combustion event, thereby increasing the fuel derived portion of the SOF.

5) Engine load has an effect on particulate emission rate and composition. At higher loads, the SOF is reduced. The greatest total particulate rate is at low load, while the medium load condition created the lowest rate. This suggests that the chosen high load condition may have been slightly over-fueled.

6) Due to the large relative effect of ring rotation, a single cylinder engine may not be the best experimental device for measuring relative changes in particulate emissions. Multi-cylinder engines will reduce the effect of individual ring rotations; presumably the effects of rotations in all the cylinders would mask individual cylinder changes.

Chapter 8 RECOMMENDATIONS

8.1 Sampling System and Procedural Improvements

Various improvements can be made to the system developed in this study to improve the quality of future study. Measurement of dilution ratio is of prime concern. Confirmation of the carbon dioxide sampling method using flowrates could confirm the reliability of this method. The use of the entire engine exhaust in a larger dilution tunnel would allow more dilution air to be used. Higher flowrates would increase sensitivity, as changes to pressure using the control valve would have a smaller relative effect. A larger dilution tunnel would also reduce the effect of build-up on the side of the tunnel, an effect which is otherwise difficult to control or measure.

Another possibility is the replacement of the compressed air source with a constant volume blower. If such a blower were used, the dilution air flowrate would be constant, allowing for direct measurement of dilution ratio.

For better consistency, it is desirable to measure liner temperature directly, in addition to measuring coolant temperature. Because this factor has a significant effect on oil volatility, it must be kept constant between tests.

8.2 Future Study

This study attempts to improve the understanding of the mechanisms and factors surrounding particulate emissions. In a broader sense, it also attempts to strengthen the relationships between oil consumption, particulate composition, and particulate emission rate. This study makes indirect conclusions about the relationship between oil consumption and particulate rate based on the particulate rate and composition data.

Better analysis would also include direct consumption measurement using a radio tracer or similar technique to verify the conclusions of this study. In addition, continued work on the effects of lubricant parameters on fuel derived emission would increase the understanding of mechanisms like fuel absorption.

SECTION 2: AQUEOUS EXHAUST INJECTION STUDY

Chapter 9 BACKGROUND

While much research and development has focused on the reduction of emissions from land vehicles, far less has been studied about the emissions from engines in marine applications. Ship engines can be far larger than those on land vehicles, often approaching the size of a small generating station. In addition, engines behave differently in ships. They are usually governed differently and are operated under vastly different conditions than those in cars or trucks. Many more factors determine their performance, including ship hull shape, sea state, ship load and propeller configuration.

Significant emissions test have been conducted aboard large vessels by Lloyd's Register [22]. While these tests have been comprehensive, they apply to large merchant ships, only one type of waterborne vessel. In addition, the measurement equipment is large enough so as to be impractical for smaller ship use. The U. S. Coast Guard(CG) is presently cosponsoring research with the Maritime Administration (MARAD) examining various aspects of marine diesel emissions, but predominantly as a prelude to studying the merits of alternative fuels. The work is being coordinated with five other agencies through a Federal Work Group.

The CG/MARAD project initially focused on taking exhaust measurements on 82' Coast Guard Patrol Boats (WPB) at the exit of the turbocharger using portable, small, suitcase-sized equipment. The experiments have focused on determining the overall emissions profile of the vessels and evaluating the performance of the portable emission analyzers in this setting. One drawback to these field studies, however, is the inability for the exhaust to be measured as it actually exits the ship. This is critical for this particular

class of ships, as water is injected into the exhaust well after it leaves the engine, possibly affecting the emissions substantially [23].

This marine-specific factor has not previously been studied. Such a configuration involves the spraying of water, usually waste cooling sea water, into the exhaust line. The purpose of such a design is to cool and muffle the exhaust as it travels out of the engineroom and aft through the ship. Commonly, this cooling method is found on small to medium sized ships, i.e., those too small for a vertical funnel-type stack.

The interest in aqueous exhaust injection is two-fold. First, in the effort to reduce airborne emissions, it is hoped that water spray will remove some of the exhaust products from the air, rendering the ship better able to comply with state and federal standards. Second, and somewhat contradictory to the first reason, it is desirable to know if any harmful products are dissolving or otherwise mixing in the water, in an effort to better assess the impact on the waterways.

In conjunction with the aforementioned CG/MARAD work, the purpose of this study is to preliminarily determine if aqueous exhaust injection changes the concentrations of the emissions products in the airborne exhaust. In addition, the portable emissions analyzer used in the field will be compared to the established laboratory emissions measurement equipment.

Chapter 10 EXPERIMENTAL APPARATUS

10.1 Engine

The experimental engine and test bed is the same as described in sub-chapter 3.1.

10.2 Exhaust Configuration

The aqueous injection configuration was modeled after the exhaust system on a WPB. This ship was chosen because it has a significant aqueous injection system and because extensive tests have been carried out on this class of ships by the U. S. Coast Guard R&D Center in an effort to measure the emissions compliance of this numerically large class of ships.

The WPB has two Caterpillar 3412 diesel engines. The oil and coolant on these engines are cooled by raw sea water pumped through heat exchangers by an attached pump. After completing its engine cooling task, the water is routed to the very aft bulkhead of the engineroom where it is injected into the exhaust.

The water is injected at a flange which has been specially connected to a 1' long double walled portion of the exhaust pipe. The double wall is created by an inner and outer pipe, each welded to a flange. When the flanges are bolted together, the smaller, exhaust input, pipe fits inside the larger, exhaust and water output, pipe. 1' beyond the flange, the inner pipe, which has been machined, ends in a lip which effectively makes the outer diameter of the inner wall just barely (about 1/16") smaller than the inner diameter of the outer wall. The inlet water line is then connected to the outer pipe. Water fills the chamber between the walls and is sprayed out into the exhaust, at the lip, which is traveling through the inner pipe. Figure 10-1 illustrates this configuration.

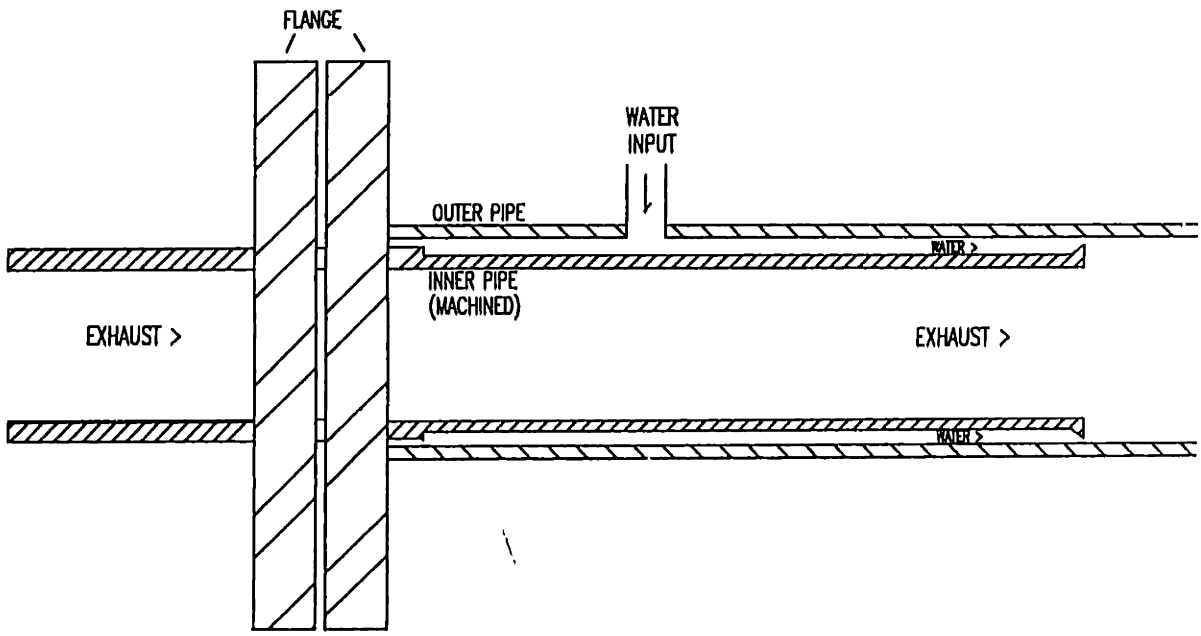

Figure 10-1 Water Injection Flange Apparatus

In the laboratory, a similar flange was machined and installed in the 2" exhaust line of the experimental engine. Figure 10-2 is a diagram of the aqueous injection apparatus. Water is supplied to the flange through 1/2" copper tubing which has a thermocouple and rotameter. The water and exhaust mixture enter an upright heated separation tank where the water is allowed to drain from the bottom and the exhaust exits through a heated exhaust line at the top of the tank. The heating serves to begin conditioning the sample for analysis. After traveling a short length of heated exhaust pipe, the exhaust passes through a sampling port, which serves as the location for after-injection sampling.

10.3 Emissions Sampling System

Emissions samples are taken from the exhaust system at any one of four locations. The sample leaves the exhaust pipe through a heated 1/2" stainless steel tube. Heating is accomplished with heat tapes wrapped around the tubing which are controlled by variable resistors. The heated tube is then enclosed within 1" PVC pipe which acts as an insulator. This sampling line acts to keep the exhaust warm and non-condensed as it travels to the measurement equipment. The heated line succeeded in keeping the exhaust sample above 140°C as it entered the measurement equipment.

For the aqueous injection study, two emissions measurement systems were used. The first was the standard apparatus used at the Sloan Automotive Laboratory. This "cart" consists of a sample vacuum pump which supplies a variety of different analyzers. The sample is drawn through a filter and ice water drier for conditioning. The oxygen analyzer uses a polarographic technique which directly measures oxygen partial pressure. The carbon monoxide and carbon dioxide use the infrared radiation technique to make measurements. The NO_X analyzer measures the chemiluminescence from excited NO to measure the concentration.

Simultaneously, measurements were taken using the sample portable equipment used in the CG/MARAD studies, the ENERAC 2000E. This instrument measures oxygen, carbon monoxide, nitric oxide, nitrogen dioxide, NO_X, sulfur dioxide and combustibles, using electrochemical cells. The unit includes a conditioning probe which can be inserted directly into the exhaust stream. In this case, the probe was mounted near the cart and configured to take an exhaust sample at the same place as the cart. The conditioning probe filters particulates and dries the hot exhaust using desiccant and a membrane technique.

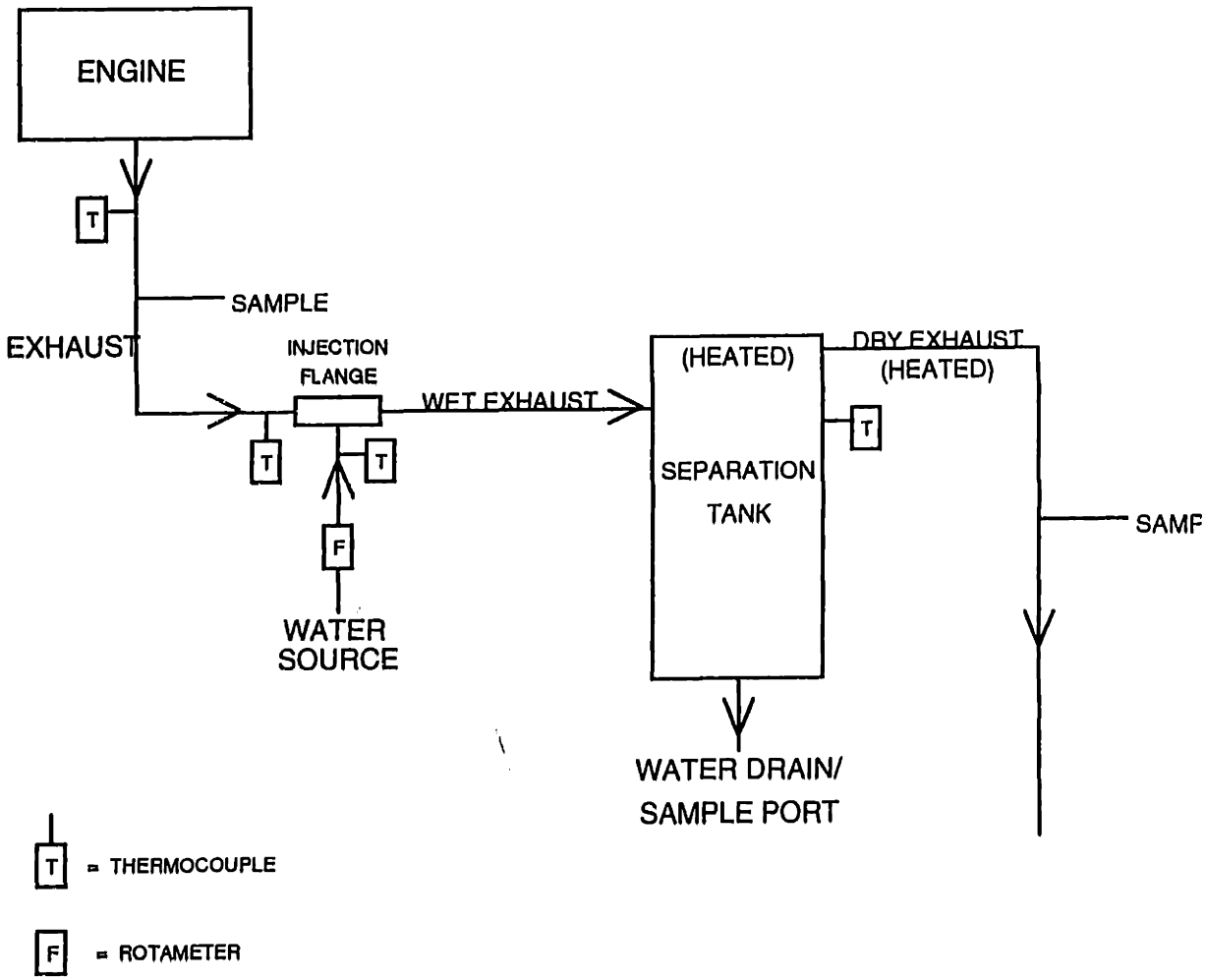

Figure 10-2 Experimental Apparatus

Chapter 11 EXPERIMENTATION

11.1 Test Procedure

The engine is started and warmed. Water is supplied to the exhaust flange and sprays into the exhaust. All system heaters are turned on and allowed to stabilize. When the proper water flowrate is set using the rotameter and the engine and sampling system temperatures are stabilized at the first operating condition, data are taken. In addition to engine data, all sampling system temperatures are recorded. Finally, gaseous emissions readings are taken immediately after the exhaust manifold and again after the water/exhaust separation tank. An 8 fl. oz. water sample is collected in a glass bottle at the tank drain. After each round of data, the engine is brought to the new operating condition per the test matrix and allowed to stabilize at the new condition.

11.2 Controls

Every effort was made to keep temperatures constant from test to test of the same operating condition. Between each test, the engine was given sufficient time to stabilize. The temperature of the emissions sample entering the measurement instruments was the same for both the "before" and "after" samples.

The injected water to exhaust mass flowrate ratio was kept constant at 10:1 for all operating conditions, except the one where it was intentionally altered as a variable and set at 30:1. This ratio was kept constant to allow the same relative amount of mixing between the exhaust and water so that two tests from different operating conditions with different absolute flowrates could be compared. The 10:1 value was used as it

approximates the water to mass flowrate ratio found on the WPB during a common operating condition.

11.2 Test Matrix

OPERATING CONDITION	INJECTED WATER/EXHAUST MASS FLOWRATE RATIO	# OF TESTS
A	10	5
B	10	5
C	10	5
F	30	5
D	10	5
E	10	5

Table 11-1 Operating Conditions

Two variables were used for this study, namely engine operating condition and injection water to exhaust mass flowrate ratio. Table 11-1 defines the operating conditions. Each test was run five times in a random sequence for repeatability. Table 11-2 outlines the test matrix.

CONDITION	SPEED (RPM)	LOAD	FUEL FLOW (CC/MIN)
A	1200	MEDIUM	9.7
B	2400	MEDIUM	19.4
C	2400	HIGH	25.8
D	3600	MEDIUM	39.1
E	3600	HIGH	56.0

Table 11-2 Test Matrix

The injected water to exhaust mass flowrate ratio was chosen to be 10 for the majority of the tests. This value was calculated from WPB engine data as an approximate average of the ratio in the exhaust system. To see if this flowrate ratio is a factor in the emissions reduction, one round of tests with condition C were run with a ratio three times larger.

Chapter 12 THEORY

One primary purpose of this research is to study the reduction of NOx emissions using aqueous exhaust injection. This chapter will develop a theoretical prediction of the solubility of nitric oxide in the injected water.

First, the saturated concentration of nitric oxide in the injected water must be calculated. For these calculations, data will be used from operating condition C. In this condition, the temperature of the water at the separation tank exit is 10°C. The solubility of nitric oxide in water at 10°C is [24]:

$$\overline{x} = .0000458 \qquad (12\text{-}1)$$

where:

$\overline{x}$ = the saturated mole fraction of NO in water

The mass flowrate of water is known. From that, the molar flowrate of water can be calculated and multiplied by the solubility mole fraction to obtain the maximum molar rate at which NO can dissolve in the water:

$$\dot{x}_{NO} = \frac{\left(\dot{m}_{H_2O}\right)\left(\overline{X}\right)}{MW_{H_2O}} \qquad (12\text{-}2)$$

where:

MW_{H2O} = molecular weight of water = 18

$\dot{x}_{NO}$ = saturated mass flowrate of nitric oxide = 0.01528 mol/min

$\dot{m}_{H_2O}$ = water mass flowrate = 6008.4 g/min

Knowing the exhaust mass flowrate and the exhaust molecular weight, the molar flowrate of the exhaust can be calculated. From this information and the saturated mass

flowrate of nitric oxide, the maximum reduction of nitric oxide due to dissolution in water, can be calculated:

$$R_m = \frac{\left(\dot{x}_{NO}\right)\left(MW_{ex}\right)}{\dot{m}_{ex}} \qquad (12\text{-}3)$$

where:

R_m = maximum(saturated) removal rate of NO = 737 ppm
MW_{ex} = exhaust molecular weight = 29.01
$\dot{m}_{ex}$ = exhaust mass flowrate = 600.84 g/min

Saturation rate, however, is a function of time and amount of mixing. In the laboratory, the nitric oxide and water are only in contact for less than five seconds. In addition, there are other compounds present which may affect the solution rate or solubility of the gas. To account for this, the mixing factor is introduced, which must be determined empirically for each exhaust configuration, and is a function of contact time and mixing phenomenon:

$$R_a = R_m f_{mix} \qquad (12\text{-}4)$$

where:

R_a = actual removal rate of NO
f_{mix} = mixing factor (empirically determined)

Therefore, these calculations predict a maximum removal (f_{mix} = 1) of 737 ppm from the exhaust at operating condition C. Presumably, the actual removal rate will be something less.

Chapter 13 RESULTS

13.1 Gaseous Emissions

As stated in Chapter 11, gaseous emissions were measured upstream and downstream of the aqueous injection by two independent instruments. The entire collection of specific results are included in appendix C.

The absolute results and trends measured by these instruments did not at all agree. While the ENERAC measured little change in emission levels created by injection, the gas cart showed there to be significant differences at conditions D, E, and F. Careful analysis of these results show a consistent increase in oxygen and a consistent decrease in carbon dioxide, carbon monoxide and oxides of nitrogen concentrations. While such changes are not predicted and the ENERAC did not measure any such relative differences, the changes measured by the gas cart are most likely due to a small leak before the intake to the vacuum pump. Such a leak would not be detected by the normal calibration procedures as the span gas enters the detection stream under positive pressure. In addition, at the higher speeds and loads of conditions D, E, and F, the exhaust leaving the engine at the manifold is under high enough pressure for the inlet side of the gas cart vacuum pump to be pressurized, whereas after water injection, the exhaust pressure is sufficiently low so as to allow a vacuum to develop before the vacuum pump. At the lower speed and load conditions, both the before and after injection measurements were at sufficiently low pressure for ambient air to be drawn into the sample, therefore a difference in concentration would not be detected as in the other conditions.

Based on these results and analyses, for this portion of the studies, only the ENERAC results will be used to draw conclusions about the effects of aqueous exhaust injection. At all conditions, no significant differences were noted in the concentrations of

Gas	Condition	Mean Absolute Change	Σ Absolute Change	% Change
CO (ppm)	A	-57.0	111.4	-4.1
	B	-1.8	9.6	-0.2
	C	-19.4	39..4	-2.2
	D	44.0	25.9	1.8
	E	NO RESULTS		
	F	-17.0	20.9	-2.3
O_2 (%)	A	0.00	0.2	0.2
	B	0.04	0.1	0.3
	C	0.18	.5	2.1
	D	-0.10	0.0	-0.8
	E	-0.02	6.4	-2.5
	F	0.00	0.1	0.0
NO (ppm)	A	-19.0	7.0	-3.5
	B	-8.4	5.6	-1.8
	C	3.8	6.9	0.6
	D	-8.6	5.7	-1.8
	E	-10.0	6.4	-2.5
	F	-15.0	6.2	-2.2
NO_2 (ppm)	A	3.0	5.8	4.5
	B	0.4	2.9	0.7
	C	3.8	2.5	4.8
	D	-0.2	2.6	-0.5
	E	0.4	1.5	4.2
	F	-4.0	2.1	-4.3

Table 13-1 Summary of Gaseous Emissions Results

carbon monoxide, oxygen, or nitrogen dioxide. While nitric oxide concentration reduced in five of the six conditions, the changes were not significant. Table 13-1 summarizes the average change in each of the measured gas concentrations while figure 13-1 displays the insignificant NO reduction trend. It should also be noted that the mass flowrate ratio does seem to have a small effect, as the reduction in NO was slightly greater in condition F than in condition C. This change, however, was also insignificant.

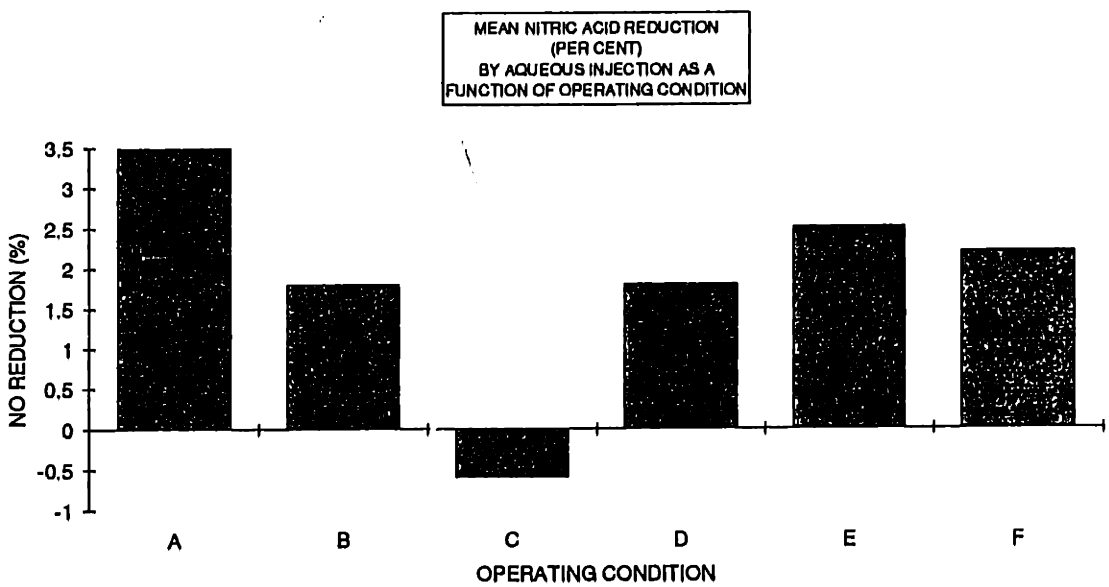

Figure 13-1 Nitric Oxide Reduction

13.2 Water Sample Analysis

At each operating condition, water samples were taken from the drain at the separation tank to assess if any of the emissions products became dissolved or otherwise mixed in the water. Original plans were to analyze these samples for indications of NO dissolved in the water. Visual inspection of the samples, however, changed this focus.

After taking the samples, it became visually clear that particulates and hydrocarbons are trapped in the water and flushed into the water column. Particulates and liquid hydrocarbons were plainly visible in the water sample, especially at the higher load conditions, where it seemed water contamination was extreme. With these unexpected observations, the samples were sent the to the sponsor's laboratory, at the U. S. Coast Guard R&D center for a hydrocarbon analysis using gas chromatography. The results of these tests were not complete in time to be included in this report.

While the initial focus of this study was the reduction of NOx emissions, it seems a significant revelation about the nature of marine diesel particulate emissions was made.

13.3 Validation of the Portable Measurement Equipment

Throughout testing during both phases of this report, emissions measurements were taken on both instruments in an effort to validate the use of portable equipment in the field. Comparison between the instruments was never good. Much of this inconsistency is most likely due to system vacuum leak, as discussed in the previous section. Because span gas calibrations indicated properly operating equipment, the leak diagnosis was not made until detailed studies of the data were made and testing was complete.

Throughout the studies, gas cart oxygen levels read higher and NOx levels were lower. If the system was being contaminated with outside air, these discrepancies would make sense. Oxygen calibrations found both to be reading correctly throughout the tests. Similarly, NOx span gas validations for the gas cart were similarly correct.

Based on these findings, it is not possible to conclude that the portable equipment performs to the same absolute or relative standard than the M.I.T. gas cart. This

statement does not in any way intend to criticize the ENERAC performance, as it was most likely the failure of the gas cart that complicated the comparison.

Chapter 14 DISCUSSION

14.1 Conclusions

Aqueous injection does not significantly affect the airborne concentration of carbon monoxide or oxides of nitrogen in laboratory measured diesel engine exhaust. The injected water does, however, capture particulate matter and presumably flush it into the body of water in which the ship is operating. While this study did not quantify this effect, visual inspection of the water samples indicated that the amount is significant.

While the intended numerical validation of the portable equipment was not conclusive, the prospects for the continued use of the equipment is promising. The results were always reasonable while the instrument responded properly to span gas calibration procedures.

14.2 Recommendations

Before further study, equipment issues need to be addressed. It is most probable that the gas cart suffers from a leak in the vacuum pump seals or immediately before it. Because it is not detectable with pressurized span gases, significant thought and diagnostic work should be expended to find and repair the leak.

To improve the situation, shorter sampling lines should be used to minimize pressure losses and allow the exhaust sample to reach the cart somewhat pressurized. This would minimize the effect of leakage.

Further study of the particulate issue would be a logical and useful continuation of these experiments. Quantification and additional chemical analysis of the particulate matter collected (from the water and air) before and after aqueous injection would not

only shed light on how much matter is removed from the exhaust, but what types of compounds are affected by the sudden cooling effect of water. This could lead to further understanding of particulate formation mechanisms and possible particulate reduction techniques in all diesel engines.

REFERENCES

1. Johnson, J. H., Bagely, S. T., Gratz, L. D., and Leddy, D. G., "A Review of Diesel Particulate Control Technology and Emissions Effects - 1992 Horning Memorial Award Lecture," SAE Paper 940233, 1994.

2. Heywood, J. B., Internal Combustion Engine Fundamentals, McGraw-Hill Book Company, New York, 1988.

3. Walsh, M. P., "Global Trends in Diesel Particulate Control," SAE Paper 930126, 1993.

4. Mayer, W. J., Lechman, D. C., and Hilden, D. L., "The Contribution of Oil to Diesel Particulate Emissions," SAE Paper 800256, 1980.

5. Hilden, D. L., and Mayer, W. J., "The Contribution of Engine Oil to Particulate Exhaust Emissions from Light Duty Powered Vehicles," SAE Paper 841395, 1984.

6. Dowling, M., "The Impact of Oil Formulation on Emissions from Diesel Engines," SAE Paper 922198, 1992.

7. Essig, G., Kamp, H., and Wacker, E., "Diesel Engine Emissions Reduction - The Benefits of Low Oil Consumption Design," ASE Paper 900591, 1990.

8. Jakobs, R. J. and Westbrooke, K., "Aspects of Influencing Oil Consumption in Diesel Engines for Low Emissions," SAE Paper 900587, 1990.

9. Andrews, G. E., Abdelhalim, S., and P. T. Williams, "The Influence of Oil Age on Emissions from an IDI Diesel," SAE Paper 931003

10. Zelenka, P., Kriegler, W., Herzog, P. L., and Cartellieri, W. P., "Ways Toward th Clean Heavy-Duty Diesel," SAE Paper 900602

11. Deutsch, E. J., "Piston Ring Friction Analysis from Oil Film Thickness Measurements," Masters Thesis, Department of Mechanical Engineering, Massachusetts Institute of Technology, 1994.

12. Hoult, D. P. and Shaw, B. T., "The Puddle Theory of Oil Consumption," Tribology Transactions, Vol 34,1,1994.

13. The Ricardo/Cussons Standard Hydra Engine and Test Bed - Instruction Manual, G. Cussons, Ltd., Manchester, England.

14. Wong, V. W., Yu, M. L., Mogaka, Z. N., and Shahed, S. M., "Effects of Catalytic Wire-Mesh Traps on the Level and Measurement of Heavy-Duty Diesel Particulate Emissions," SAE Paper 840172, 1984.

15. EPA, Code of Federal Regulations(CFR 40), 1990.

16. Ortech Proposal # 94-E14-7123/FI, Ortech Corporation, Mississauga, Ontario, 1994.

17. Hartman, R. M., "Tritium Method Oil Consumption and Its Relation to Oil Film Thickness in a Production Diesel Engine," Masters Thesis, Department of Mechanical Engineering, Massachusetts Institute of Technology, 1990.

18. 1994 Shell Lubricants Handbook, Shell Oil Company, 1994.

19. "Fuel/Lube Contribution Analysis Procedure," Cummins Engine Company, 1994.

20. Norris, Michael, Private Conversation, Sloan Automotive Laboratory, Massachusetts Institute of Technology, May, 1994.

21. Schneider, E. W. and Blossfeld, D. H., "Method for Measurement of Piston Ring Rotation in an Operating Engine," SAE Paper 900224, 1990.

22. "Marine Exhaust Emissions Research Programme - Steady State Operation," Lloyds Register of Shipping, 1990-1993.

23. Bentz, Dr. Alan P., Private Phone Conversation, U. S. Coast Guard Research and Development Center, Groton, CT, 1994

24. Gerrard, William, Gas Solubilities, Pergamon Press Ltd., Oxford, 1980.

Appendix A PARTICULATE RATE RESULTS

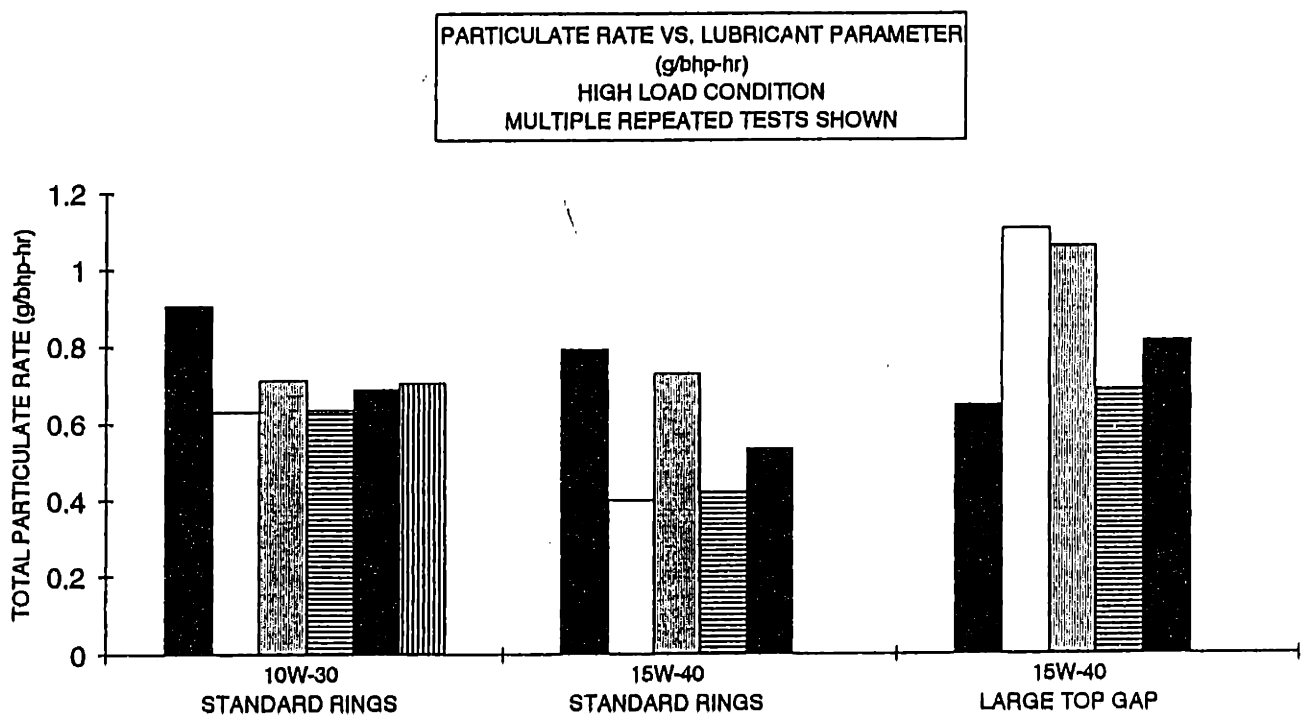

Figure A-1 Individual Particulate Rate Test Results - High Load Condition

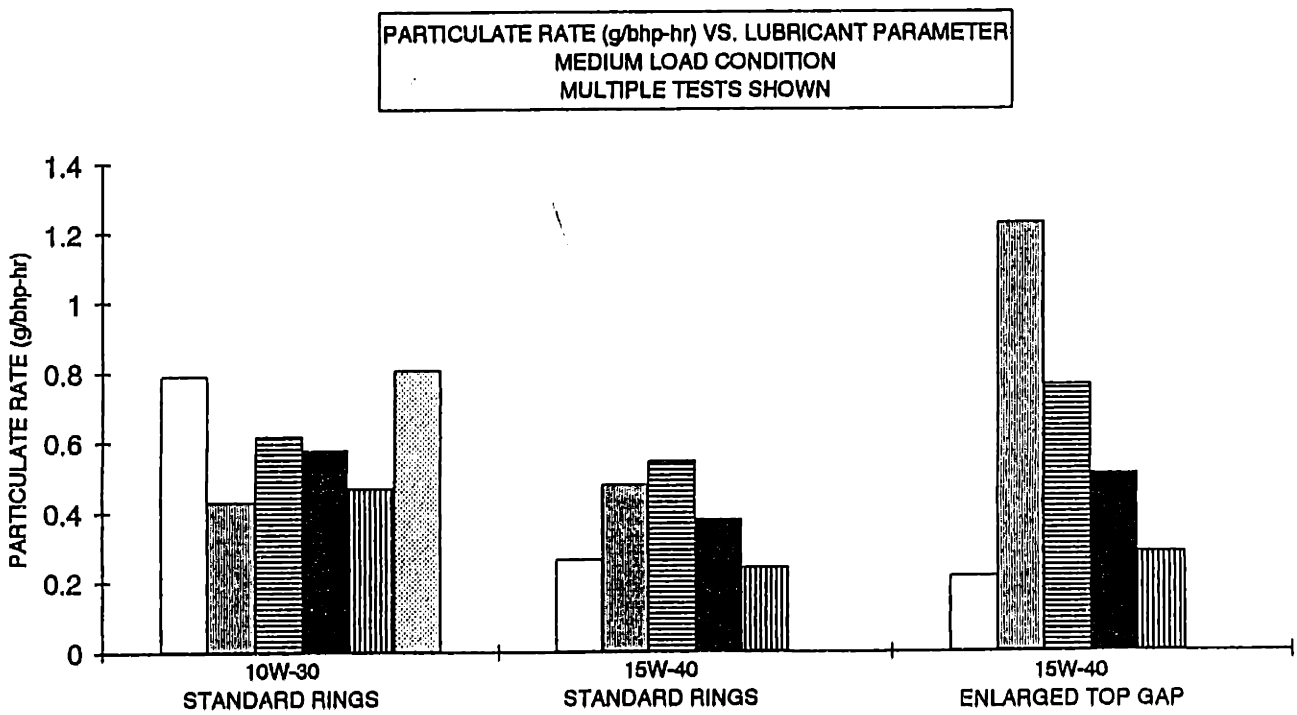

Figure A-2 Individual Particulate Rate Test Results - Medium Load Condition

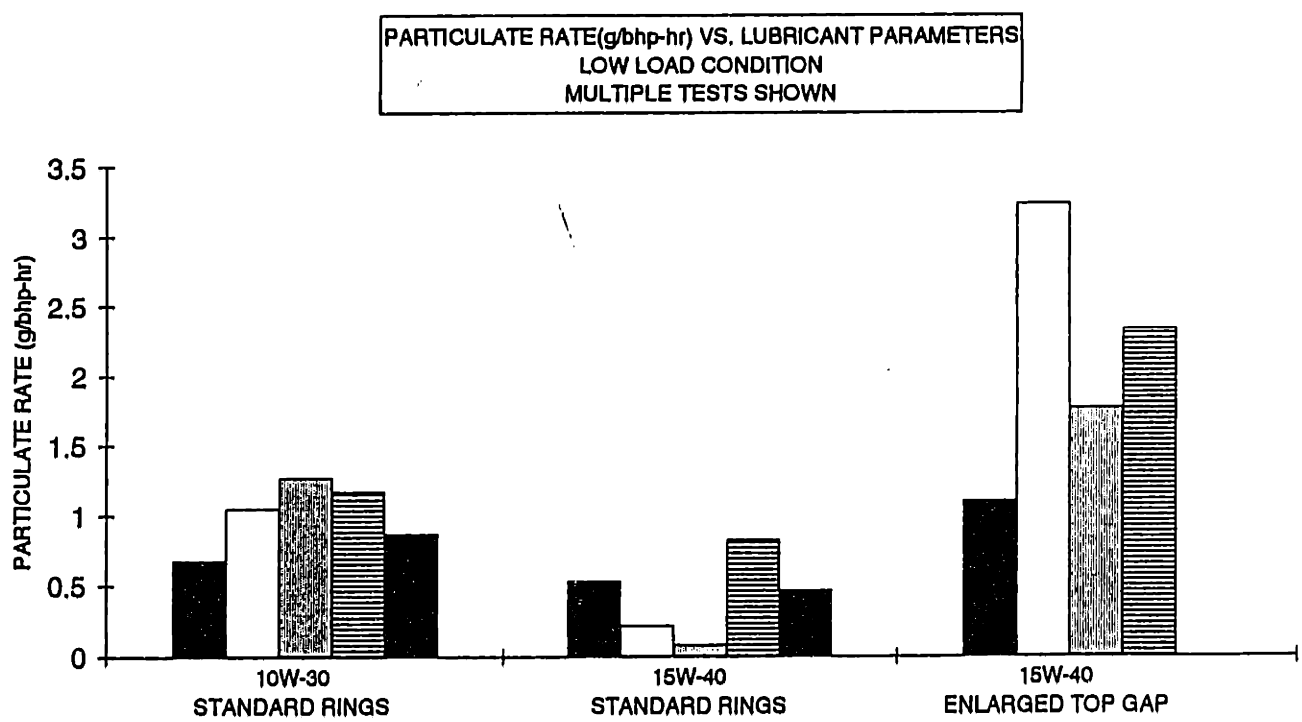

Figure A-3 Individual Particulate Rate Test Results - Low Load Condition

Appendix B SOF RESULTS

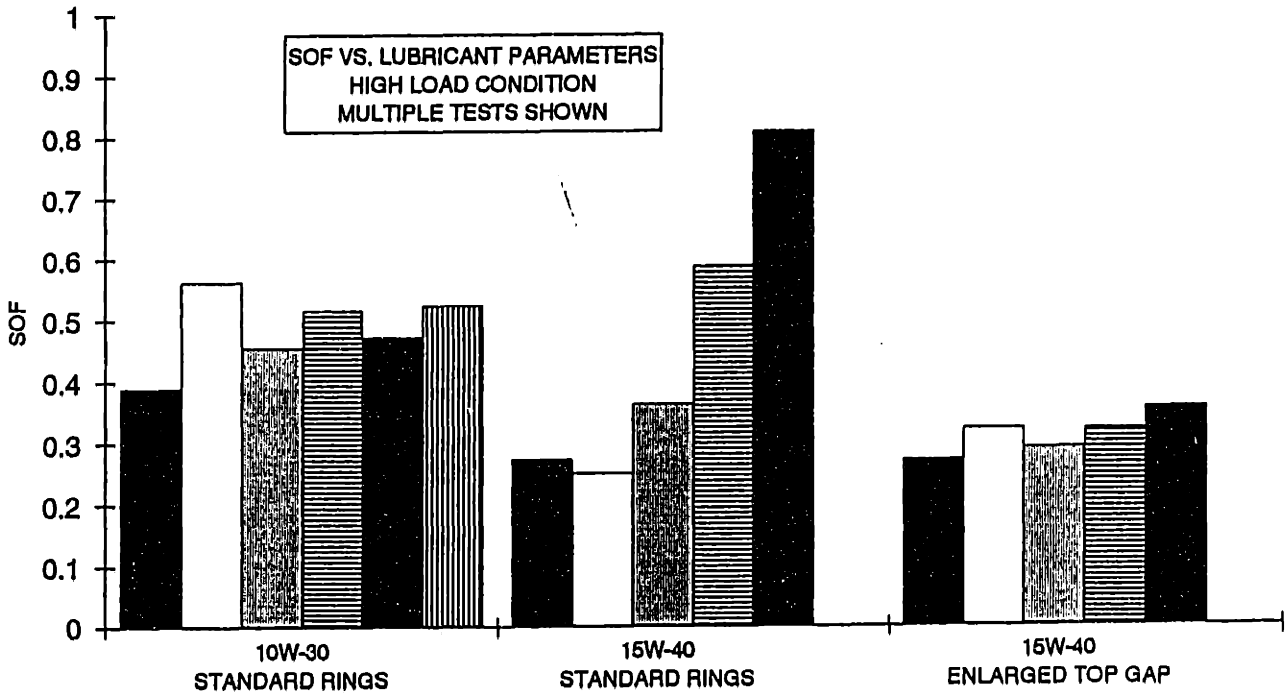

Figure B-1 Individual SOF Test Results - High Load Condition

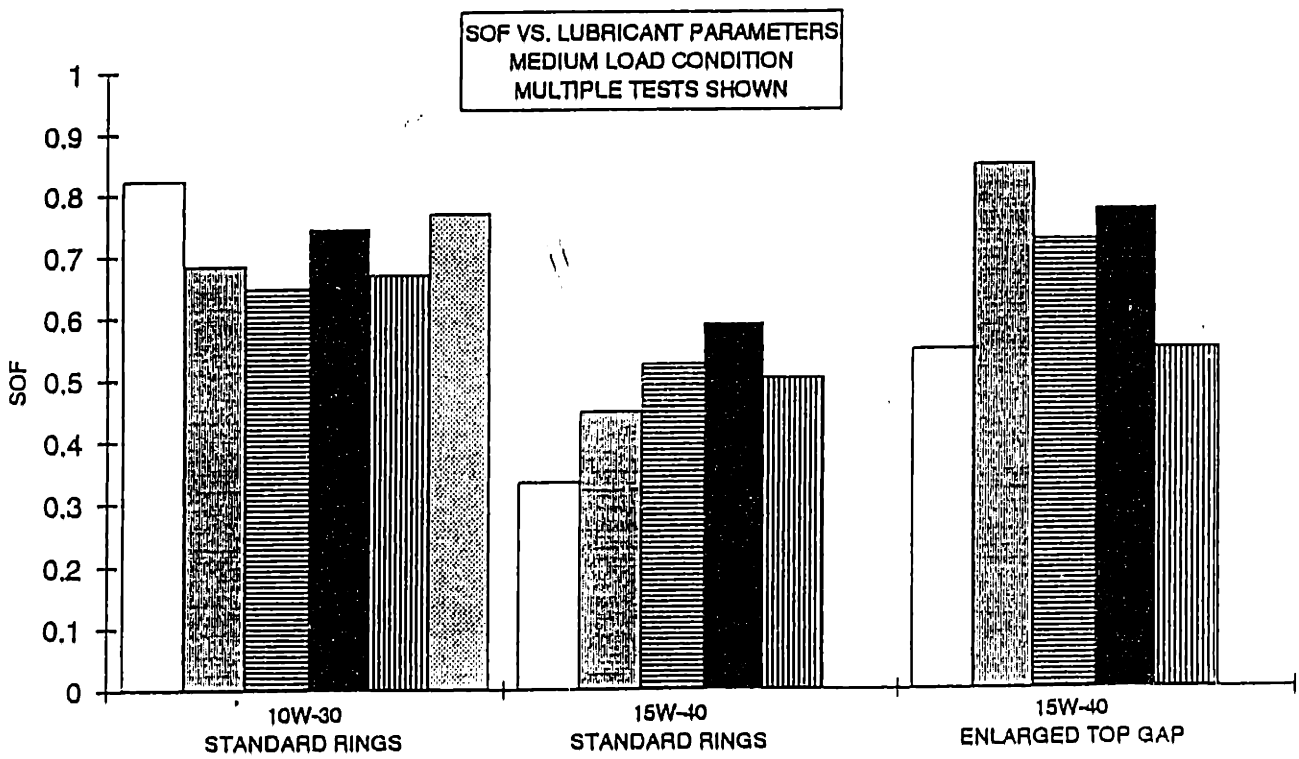

Figure B-2 Individual SOF Test Results - Medium Load Condition

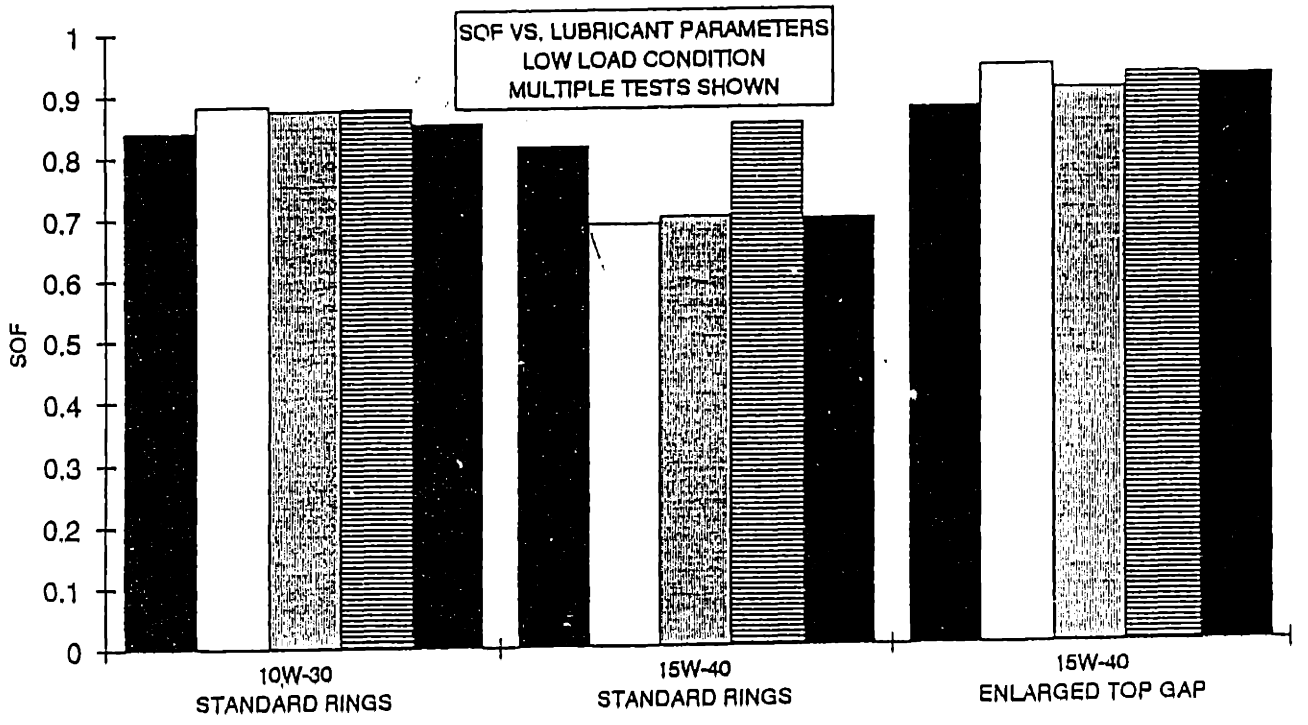

Figure B-3 Individual SOF Test Results - Low Load Condition

Appendix C AQUEOUS INJECTION RESULTS

TEST #		1	8	15	20	22	MEAN	STDEV	% CHG
			ENERAC	RESULTS					
CO ppm	BEFORE	1551	1793	1409	1346	739	1368		
	AFTER	1557	1795	1141	1280	782	1311		
	CHANGE	6	2	-268	-66	43	-57	111.4	4.1
O2 %	BEFORE	11.8	11.8	12.0	12.0	12.2	11.9		
	AFTER	11.5	11.8	12.3	12.0	12.1	11.9		
	CHANGE	-0.3	0.0	0.3	0.0	-0.1	0.0	0.2	0.2
NO ppm	BEFORE	541	507	552	545	597	548		
	AFTER	520	496	525	534	571	529		
	CHANGE	-21	-11	-27	-11	-26	-19	7.0	3.5
NO2 ppm	BEFORE	79	55	86	70	90	76		
	AFTER	79	61	99	72	86	79		
	CHANGE	0	6	13	2	-4	3	5.8	4.5
NOX ppm	BEFORE	619	562	637	615	686	624		
	AFTER	599	566	623	606	657	610		
	CHANGE	-20	4	-14	-9	-29	-14	11.0	2.2
			GAS CART	RESULTS					
CO2 %	BEFORE	2.53	1.83	2.25	2.64	2.53	2.36		
	AFTER	2.25	1.35	1.39	1.94	1.63	1.71		
	CHANGE	-0.28	-0.48	-0.86	-0.70	-0.90	-0.64	0.2	27.3
CO %	BEFORE	0.06	0.07	0.05	0.08	0.05	0.06		
	AFTER	0.05	0.06	0.05	0.07	0.05	0.06		
	CHANGE	-0.01	-0.01	0.00	-0.01	0.00	-0.01	0.0	9.7
O2 %	BEFORE	15.7	16.5	16.5	16.8	16.7	16.4		
	AFTER	15.8	16.8	17.1	17.0	17.6	16.9		
	CHANGE	0.1	0.3	0.6	0.4	0.9	0.5	0.3	2.8
NOX ppm	BEFORE	230	215	200	260	355	252		
	AFTER	245	195	205	240	260	229		
	CHANGE	15	-20	5	-20	-95	-23	38.5	9.1

Figure C-1 Aqueous Exhaust Injection - Gasseous Emission Results - Condition A

TEST #		2	9	14	19	23	MEAN	STDEV	% CHG
			ENERAC	RESULTS					
CO	BEFORE	1096	755	794	686	680	802.2		
	AFTER	1087	757	789	701	668	800.4		
ppm	CHANGE	-9	2	-5	15	-12	-1.8	9.6	0.2
O2	BEFORE	12.1	12.2	12.7	13.2	12.6	12.56		
	AFTER	12.1	12.4	12.7	13.2	12.6	12.6		
%	CHANGE	0	0.2	0	0	0	0.04	0.1	0.3
NO	BEFORE	457	461	478	455	469	468		
	AFTER	454	442	473	447	462	459.6		
ppm	CHANGE	-3	-19	-5	-8	-7	-8.4	5.6	1.8
NO2	BEFORE	62	48	65	52	62	57.8		
	AFTER	60	46	71	52	62	58.2		
ppm	CHANGE	-2	-2	6	0	0	0.4	2.9	0.7
NOX	BEFORE	518	509	542	507	551	525.4		
	AFTER	513	487	543	498	544	517		
ppm	CHANGE	-5	-22	1	-9	-7	-8.4	7.6	1.6
			GAS CART	RESULTS					
CO2	BEFORE	2.58	1.99	1.94	2.58	2.47	2.312		
	AFTER	2.36	1.73	1.54	2.14	2.09	1.972		
%	CHANGE	-0.22	-0.26	-0.4	-0.44	-0.38	-0.34	0.1	14.7
CO	BEFORE	0.04	0.06	0.04	0.07	0.05	0.052		
	AFTER	0.05	0.06	0.04	0.07	0.05	0.054		
%	CHANGE	0.01	0	0	0	0	0.002	0.0	3.8
O2	BEFORE	16.5	16.5	16.7	16.8	16.7	16.4		
	AFTER	16.6	16.6	17	17	17.1	16.66		
%	CHANGE	0.1	0.1	0.3	0.4	0.4	0.26	0.1	1.6
NOX	BEFORE	230	215	190	285	295	243		
	AFTER	245	200	200	245	250	228		
ppm	CHANGE	15	-15	10	-40	-45	-15	24.7	6.2

Figure C-2 Aqueous Exhaust Injection - Gasseous Emission Results - Condition B

TEST #		3	7	12	18	25	MEAN	STDEV	% CHG
			ENERAC	RESULTS					
CO	BEFORE	1267	1041	664	631	669	894.4		
	AFTER	1230	1019	707	627	792	875		
ppm	CHANGE	-37	-22	43	-4	-77	-19.4	39.4	2.2
O2	BEFORE	8.3	8.5	9	8.9	8.5	8.64		
	AFTER	9.5	8.3	8.8	8.9	8.6	8.82		
%	CHANGE	1.2	-0.2	-0.2	0	0.1	0.18	0.5	2.1
NO	BEFORE	639	618	681	671	671	656		
	AFTER	639	633	686	665	676	659.8		
ppm	CHANGE	0	15	5	-6	5	3.8	6.9	0.6
NO2	BEFORE	73	68	97	87	75	80		
	AFTER	75	73	104	87	80	83.8		
ppm	CHANGE	2	5	7	0	5	3.8	2.5	4.8
NOX	BEFORE	711	685	778	758	745	735.4		
	AFTER	713	706	790	752	756	743.4		
ppm	CHANGE	2	21	12	-6	11	8	9.2	1.1
			GAS CART	RESULTS					
CO2	BEFORE	4.63	3.42	3.8	5	4.42	4.254		
	AFTER	4.42	2.93	3.67	4.28	3.74	3.808		
%	CHANGE	-0.21	-0.49	-0.13	-0.72	-0.68	-0.446	0.2	10.5
CO	BEFORE	0.06	0.06	0.04	0.07	0.07	0.06		
	AFTER	0.05	0.05	0.05	0.07	0.07	0.058		
%	CHANGE	-0.01	-0.01	0.01	0	0	-0.002	0.0	3.3
O2	BEFORE	13.8	15.2	14.7	14.8	15	14.88		
	AFTER	14	15.6	15	15.2	15.5	15.06		
%	CHANGE	0.2	0.4	0.3	0.6	0.5	0.4	0.1	2.7
NOX	BEFORE	315	250	300	340	410	323		
	AFTER	380	275	295	395	370	343		
ppm	CHANGE	65	25	-5	55	-40	20	38.7	6.2

Figure C-3 Aqueous Exhaust Injection - Gasseous Emission Results - Condition C

TEST #		4	10	11	17	24	MEAN	STDEV	% CHG
			ENERAC	RESULTS					
CO	BEFORE	3168	2764	2375	1807	1835	2389.8		
	AFTER	3233	2780	2384	1868	1904	2433.8		
ppm	CHANGE	65	16	9	61	69	44	25.9	1.8
O2	BEFORE	7.7	7.7	8	8	8.2	7.92		
	AFTER	7.8	7.7	7.9	8	8.1	7.88		
%	CHANGE	-0.1	0	-0.1	0	-0.1	-0.06	0.0	0.8
NO	BEFORE	440	458	500	496	501	479		
	AFTER	434	445	501	481	491	470.4		
ppm	CHANGE	-6	-13	1	-15	-10	-8.8	5.7	1.8
NO2	BEFORE	34	30	46	42	42	38.8		
	AFTER	36	30	49	38	40	38.6		
ppm	CHANGE	2	0	3	-4	-2	-0.2	2.6	0.5
NOX	BEFORE	474	488	546	537	543	517.6		
	AFTER	469	474	550	519	531	508.6		
ppm	CHANGE	-5	-14	4	-18	-12	-9	7.7	1.7
			GAS CART	RESULTS					
CO2	BEFORE	6.54	5.86	7.63	8.61	7.53	7.234		
	AFTER	4.07	3.67	4.56	5.86	4.28	4.488		
%	CHANGE	-2.47	-2.19	-3.07	-2.75	-3.25	-2.746	0.4	38.0
CO	BEFORE	0.13	0.14	0.13	0.14	0.13	0.134		
	AFTER	0.1	0.11	0.1	0.12	0.09	0.104		
%	CHANGE	-0.03	-0.03	-0.03	-0.02	-0.04	-0.03	0.0	22.4
O2	BEFORE	12.4	13.1	11.8	11.5	12.3	12.18		
	AFTER	14.4	14.9	14.2	14	15.2	14.54		
%	CHANGE	2	1.8	2.6	2.5	2.9	2.36	0.4	19.4
NOX	BEFORE	330	305	320	350	425	346		
	AFTER	230	215	250	325	275	259		
ppm	CHANGE	-100	-90	-70	-25	-150	-87	40.7	25.1

Figure C-4 Aqueous Exhaust Injection - Gasseous Emission Results - Condition D

TEST #		5	6	13	16	21	MEAN	STDEV	% CHG
			ENERAC	RESULTS					
CO	BEFORE	OVER	OVER	OVER	OVER	OVER	OVER		
	AFTER	OVER	OVER	OVER	OVER	OVER	OVER		
	CHANGE							#DIV/0!	#VALUE!
O2	BEFORE	1.4	1.4	2.1	1.9	2.3	1.82		
	AFTER	1.4	1.4	2.3	1.8	2.1	1.8		
	CHANGE	0	0	0.2	-0.1	-0.2	-0.02	0.1	1.1
NO	BEFORE	367	365	451	410	446	407.8		
	AFTER	353	351	436	412	437	397.8		
	CHANGE	-14	-14	-15	2	-9	-10	8.4	2.5
NO2	BEFORE	8	6	13	10	11	9.6		
	AFTER	6	8	15	10	11	10		
	CHANGE	-2	2	2	0	0	0.4	1.5	4.2
NOX	BEFORE	374	370	464	419	457	416.8		
	AFTER	359	358	451	421	448	407.4		
	CHANGE	-15	-12	-13	2	-9	-9.4	8.0	2.3
			GAS CART	RESULTS					
CO2	BEFORE	9.24	9.67	12.02	14.42	12.4	11.55		
	AFTER	5.38	5.86	6.62	9.67	7.16	6.938		
	CHANGE	-3.86	-3.81	-5.4	-4.75	-5.24	-4.612	0.7	39.9
CO	BEFORE	0.64	0.64	0.44	0.53	0.43	0.536		
	AFTER	0.44	0.44	0.27	0.41	0.27	0.366		
	CHANGE	-0.2	-0.2	-0.17	-0.12	-0.16	-0.17	0.0	31.7
O2	BEFORE	9.7	9.7	7.7	5.8	7.5	8.08		
	AFTER	13.5	13.5	12.5	10.7	12.7	12.58		
	CHANGE	3.8	3.8	4.8	4.9	5.2	4.5	0.6	55.7
NOX	BEFORE	220	280	290	450	300	308		
	AFTER	160	175	230	295	230	218		
	CHANGE	-60	-105	-60	-155	-70	-90	36.5	29.2

Figure C-5 Aqueous Exhaust Injection - Gasseous Emission Results - Condition E

TEST #		26	27	28	29	30	MEAN	STDEV	% CHG
			ENERAC	RESULTS					
CO ppm	BEFORE	793	786	748	746	701	773		
	AFTER	802	746	745	737	747	755		
	CHANGE	9	-40	-3	-9	-44	-17	20.9	2.3
O2 %	BEFORE	8.5	8.7	8.7	8.7	8.7	8.7		
	AFTER	8.6	8.6	8.7	8.7	8.7	8.7		
	CHANGE	0.1	-0.1	0.0	0.0	0.0	0.0	0.1	0.0
NO ppm	BEFORE	686	684	684	689	677	684		
	AFTER	668	681	668	670	657	669		
	CHANGE	-18	-3	-16	-19	-20	-15	8.2	2.2
NO2 ppm	BEFORE	82	84	84	86	82	84		
	AFTER	77	84	80	80	79	80		
	CHANGE	-5	0	-4	-6	-3	-4	2.1	4.3
NOX ppm	BEFORE	767	767	768	774	759	767		
	AFTER	744	765	748	750	736	749		
	CHANGE	-23	-2	-20	-24	-23	-18	8.3	2.4
			GAS CART	RESULTS					
CO2 %	BEFORE	5.54	5.46	4.92	5.07	5.15	5.23		
	AFTER	3.48	3.05	2.87	2.93	2.99	3.06		
	CHANGE	-2.06	-2.41	-2.05	-2.14	-2.16	-2.16	0.1	41.4
CO %	BEFORE	0.07	0.07	0.07	0.07	0.07	0.07		
	AFTER	0.07	0.07	0.07	0.07	0.07	0.07		
	CHANGE	0.00	0.00	0.00	0.00	0.00	0.00	0.0	0.0
O2 %	BEFORE	13.9	14.3	14.8	14.7	14.7	14.5		
	AFTER	15.8	16.4	16.6	16.6	16.6	16.4		
	CHANGE	1.9	2.1	1.8	1.9	1.9	1.9	0.1	13.3
NOX ppm	BEFORE	495	480	450	460	450	467		
	AFTER	340	320	310	315	310	319		
	CHANGE	-155	-160	-140	-145	-140	-148	8.1	31.7

Figure C-6 Aqueous Exhaust Injection - Gasseous Emission Results - Condition F

(This page intentionally left blank)

(This page intentionally left blank)